recognize microbial patterns and signatures and the TIR participates in intracellular signaling. The functional results for laTLR14b overexpressed in human cells are at least compatible with those for TLRs of other species. Yet, the pattern for recognition by this laTLR remains unknown. Further investigation is needed to determine whether the lamprey TLRs are localized to putative macrophages/monocytes. These cells may differ from lamprey lymphocytes, which have been shown to be VLR-positive cells.

Our data also suggest that the lamprey protein laTLR14b is capable of activating the huTLR signal pathways. In fish and chicken TLRs, their functions can be determined by a reporter assay with human cells expressing a CD4-TIR chimera or dominant negative proteins. That is, the chicken TLR2 signals the presence of lipoproteins even in the human system (34). The fish TLR5 and TLR21 recognize flagellin and poly(I:C) (19) (A. Matsuo and T. Seya, unpublished data), respectively, to induce activation of the NF-κB and IFN-β promoter in human cells (33, 34). Thus, we currently hold that human MyD88 is associated with laTLR14b-mediated NF-κB and secondary IFN-β promoter activation according to the results of chimera and dominant negative experiments. The results show the likelihood that lamprey TLRs act as pattern recognition receptors and transmit signals to downstream adapter proteins in host cells. For final confirmation, however, we must examine the protein function in a system using lamprey cell lines (which are not yet available).

The two lamprey TLRs belong to the subfamily of TLR14. laTLR14a/b most resemble each other and their TIRs are ~50% homologous to that of huTLR2. Gene duplication of TLR14 ortholog may have resulted in the two TLR14 genes in the lamprey. TLR14 and TLR2 do not appear to be duplicated in fish. However, a TLR2 pseudogene appears upstream in tandem with the functional TLR2 in the opossum, dog, and human (6). The pseudogene is probably from a duplication event before the divergence of marsupials. Likewise, a putative duplication event may have caused the two lamprey TLRs.

T. rubripes has a set of TLRs similar to those of the human and mouse (9) and orthologs of MyD88, Mal/TIRAP, and TICAM (a single gene representative of TICAM-1 and TICAM-2) (A. Matsu and T. Seya, unpublished data). The fish TLR system is structurally and functionally comparable with those of the human and mouse. Only minor functional variations appear to have occurred during evolution of the vertebrate TLR system, and the fundamental functional properties of the TLR system are conserved across fish and humans. Our present results may present a key to prove that the lamprey possesses orthologs of the mammalian TLR system and adapters.

L. japonica cells discard part of their genome during maturation (18). Their genome properties may be changed year to year. We have surveyed the mRNAs of laTLR14b and VLR for 5 years. Leukocytes of all individual lampreys expressed laTLR14 (a/b) and VLRs for all 5 years. Distributions of laTLR14b in lampreys were similar among individual fish. More limited expression of TLR14a than TLR14b was observed in all individuals tested. Thus, the laTLR14b protein, which is the ortholog of immune-related TLR, is actually expressed in the gills of live lampreys.

TLR1, 2, 6, and 10 are members of the TLR2 subfamily. In humans and mice, TLR2 recognizes diacylated mycoplasma lipoproteins in combination with TLR6 and triacylated bacterial lipoproteins together with TLR1 (25, 35, 36). If TLR14 is a member of the TLR2 subfamily, laTLR14 might recognize some microbial patterns in concert with another TLR2 member protein. Thus, we investigated whether lamprey and fish TLR14 exerts its function with huTLR2 members. However, laTLR14a/b, as well as fish TLR14, did not activate NF-κB even by coexpression with huTLR2 or other TLR2 members under the condition of stimulation with bacterial lipoproteins or other known TLR ligands (data not shown). Only a chimera version consisting of extracellular CD4 and the TIR domain of laTLR14b activates NF-κB as previously reported for huTLR4 and mouse TLR6, which activate NF-κB via their CD4-mediated dimerization (1, 22). Because TLR14 is found in *T. rubripes* (fgTLR14) (6), *D. rerio*, and *X. tropicalis* but not in human, mouse and chicken, its ligand may be a component of microorganisms in water.

The genomes of *Drosophila* and the mosquito *A. gambiae* contain ~10 Toll homologues, but only a few participate in host immunity (7, 8). Others are linked to developmental functions. Likewise, immune function could not be attributed to the single Toll homologue of *Caenorhabditis elegans* (37) and *Caenorhabditis briggsae* or to the TLRs reported in the horseshoe crab *Tachypleus tridentatus* (1). In contrast, the genome of the sea urchin *Strongylocentrotus purpuratus* abounds with TLR-containing genes, presumably >300 (6, 7). The genomes of the amphioxus *Brachiostoma floridae* and the solitary tunicate *Ciona savignyi* contain >10 TLR genes (7). The protostome and deuterostome invertebrates appear to have been differentially evolved in terms of the TLR system. The differences in the TLR system may reflect the differences in the microbial environment where each species of invertebrates survives. A critical factor for the selection of the TLR system would be infection.

It has been reported that the lamprey responds to some extent to some adjuvants (38) that we have revealed as TLR agonists. In addition, the lamprey possesses a complement-like molecule that opsonizes rabbit erythrocytes (39). Later, the lamprey had been shown to have the complement system including C3 and its activation and inactivation cascades (20, 40). Major family for complement regulatory proteins consists of short consensus repeats, and the lamprey possesses a short consensus repeat-containing complement-inhibitory protein named lacrep (20). The lamprey also expresses many C-type lectins like those in *Ciona intestinalis* (41, 42). However, whether or not the TLR pathogen-recognition system is conserved in jawless fish has remained unclear at a molecular level. Our results regarding two lamprey TLRs of the TLR2 subfamily add some pieces of knowledge to the vertebrate innate immune system. The lamprey possesses a pattern recognition system involving the complement and its regulatory systems, C-type lectins, and the TLR system as observed in higher vertebrates, including humans.

Acknowledgments

We are grateful to Dr. K. Funami, Dr. M. Shingai, M. Sasai, and K. Higuchi in our laboratory for critical discussions. Thanks are also due to Dr. H. Mitani (Tokyo University, Tokyo, Japan) for providing OL-17 cells. Dr. V. Kumar (St. Louis University, St. Louis, MO) reviewed this manuscript before submission.

Disclosures

The authors have no financial conflict of interest.

References

1. Medzhitov, R., P. Preston-Hurlburt, and C. A. Janeway. 1997. A human homologue of the *Drosophila* Toll protein signals activation of adaptive immunity. *Nature* 388: 394–397.
2. Xu, Y., X. Tao, B. Shen, T. Horng, R. Medzhitov, J. L. Manley, and L. Tong. 2000. Structural basis for signal transduction by the Toll/interleukin-1 receptor domains. *Nature* 408: 111–115.
3. Bell, J. K., I. Botos, P. R. Hall, J. Askins, J. Shiloach, D. M. Segal, and D. R. Davies. 2005. The molecular structure of the Toll-like receptor 3 ligand-binding domain. *Proc. Natl. Acad. Sci. USA* 102: 10976–11080.
4. Choe, J., M. S. Kelker, and I. A. Wilson. 2005. Crystal structure of human toll-like receptor 3 (TLR3) ectodomain. *Science* 309: 581–585.

5. Lemaitre, B., E. Nicolas, L. Michaut, J. M. Reichhart, and J. A. Hoffmann. 1996. The dorsoventral regulatory gene cassette spatzle/Toll/cactus controls the potent antifungal response in *Drosophila* adults. *Cell* 86: 973–983.
6. Roach, J. C., G. Glusman, L. Rowen, A. Kaur, M. K. Purcell, K. D. Smith, L. E. Hood, and A. Aderem. 2005. The evolution of vertebrate Toll-like receptors. *Proc. Natl. Acad. Sci. USA* 102: 9577–9582.
7. Pancer, Z., and M. D. Cooper. 2006. The evolution of adaptive immunity. *Ann. Rev. Immunol.* 24: 497–518.
8. Imler, J. L., and J. A. Hoffmann. 2002. Toll receptors in *Drosophila*: a family of molecules regulating development and immunity. *Curr. Top. Microbiol. Immunol.* 270: 63–79.
9. Oshiumi, H., T. Tsujita, K. Shida, M. Matsumoto, K. Ikeo, and T. Seya. 2003. Prediction of the prototype of the human Toll-like receptor gene family from the pufferfish *Fugu rubripes* genome. *Inununogenetics* 54: 791–800.
10. Medzhitov, R. 2001. Toll-like receptors and innate immunity. *Nat. Rev. Immunol.* 1: 135–145.
11. Uinuk-Ool, T., W. E. Mayer, A. Sato, R. Dongak, M. D. Cooper, and J. Klein. 2002. Lamprey lymphocyte-like cells express homologs of genes involved in immunologically relevant activities of mammalian lymphocytes. *Proc. Natl. Acad. Sci. USA* 99: 14356–14361.
12. Pancer, Z., C. T. Amemiya, G. R. Ehrhardt, J. Ceitlin, G. L. Gartland, and M. D. Cooper. 2004. Somatic diversification of variable lymphocyte receptors in the agnathan sea lamprey. *Nature* 430: 174–180.
13. Alder, M. N., I. B. Rogozin, L. M. Iyer, G. V. Glazko, M. D. Cooper, and Z. Pancer. 2005. Diversity and function of adaptive immune receptors in a jawless vertebrate. *Science* 310: 1970–1973.
14. Pancer, Z., N. R. Saha, J. Kasamatsu, T. Suzuki, C. T. Amemiya, M. Kasahara, and M. D. Cooper. 2005. Variable lymphocyte receptors in hagfish. *Proc. Natl. Acad. Sci. USA* 102: 9224–9249.
15. Takeda, K., T. Kaisho, and S. Akira. 2003. Toll-like receptors. *Annu. Rev. Immunol.* 21: 335–376.
16. Iwasaki, A., and R. Medzhitov. 2004. Toll-like receptor control of the adaptive immune responses. *Nat. Immunol.* 10: 987–995.
17. Overath, P., J. Ruoff, Y. D. Stierhof, J. Haag, H. Tichy, I. Dykova, and J. Lom. 1998. Cultivation of bloodstream forms of *Trypanosoma carassii*, a common parasite of freshwater fish. *Parasitol. Res.* 84: 343–347.
18. Kohno, S., Y. Nakai, S. Satoh, M. Yoshida, and H. Kobayashi. 1986. Chromosome elimination in the Japanese hagfish. *Eptatretus burgeri* (Agnatha, Cyclostomata). *Cytogenet. Cell Genet.* 41: 209–214.
19. Tsujita, T., A. Ishii, H. Tsukada, M. Matsumoto, F.-S. Che, and T. Seya. 2006. Fish soluble Toll-like receptor (TLR)5 amplifies human TLR5 response via physical binding to flagellin. *Vaccine* 24: 2193–2199.
20. Kimura, Y., N. Inoue, A. Fukui, H. Oshiumi, M. Matsumoto, M. Nonaka, S. Kuratani, T. Fujita, M. Nonaka, and T. Seya. 2004. A short consensus repeat-containing complement regulatory protein of lamprey that participates in cleavage of lamprey complement 3. *J. Immunol.* 173: 1118–1128.
21. Matsumoto, M., S. Kikkawa, M. Kohase, K. Miyake, and T. Seya. 2002. Establishment of a monoclonal antibody against human Toll-like receptor 3 that blocks double-stranded RNA-mediated signaling. *Biochem. Biophys. Res. Commun.* 293: 1364–1369.
22. Takeuchi, O., T. Kawai, H. Sanjo, N. G. Copeland, D. J. Gilbert, N. A. Jenkins, K. Takeda, and A. Akira. 1999. TLR6: A novel member of an expanding toll-like receptor family. *Gene* 231: 59–65.
23. Komura, J., H. Mitani, and A. Shima. 1988. Fish cell culture: establishment of two fibroblast-like cell lines (OL-17 and OL-32) from fins of the medaka *Oryzias latipes*. *In Vitro Cell. Dev. Biol.* 24: 294–298.
24. Inoue, N., A. Fukui, M. Nomura, M. Matsumoto, K. Toyoshima, and T. Seya. 2001. A novel chicken membrane-associated complement-regulatory protein: molecular cloning and functional characterization of a chicken membrane SCR protein. *J. Immunol.* 166: 424–431.
25. Nishiguchi, M., M. Matsumoto, T. Takao, M. Hoshino, Y. Shimonishi, S. Tsuji, O. Takeuchi, S. Akira, K. Toyoshima, and T. Seya. 2001. *Mycoplasma fermentans* lipoprotein M161Ag-induced cell activation is mediated by Toll-like receptor 2: Role of N-terminal hydrophobic portion in its multiple functions. *J. Immunol.* 166: 2610–2616.
26. Nakao, Y., K. Funami, S. Kikkawa, M. Taniguchi, M. Nishiguchi, Y. Fukumori, T. Seya, and M. Matsumoto. 2005. Surface-expressed TLR 6 participates in the recognition of diacylated lipopeptide and peptidoglycan in human cells. *J. Immunol.* 174: 1566–1573.
27. Okada, Y., H. Sawa, S. Endo, Y. Orba, T. Umemura, H. Nishihara, A. C. Stan, S. Tanaka, and K. Nagashima. 2002. Expression of JC virus (JCV) agnoprotein in progressive multifocal leukoencephalopathy (PML) brain. *Acta Neuropathol.* 104: 130–136.
28. Sunden, Y., T. Suzuki, Y. Orba, T. Umemura, M. Asamoto, K. Nagashima, S. Tanaka, and H. Sawa. 2006 Characterization and application of polyclonal antibodies that specifically recognize JC virus large T antigen. *Acta Neuropathol.* 111: 379–387.
29. Jault, C., L. Pichon, and J. Chluba. 2004. Toll-like receptor gene family and TIR-domain adapters in *Danio rerio*. *Mol. Immunol.* 40: 759–771.
30. Meijer, A. H., S. F. Gabby Krens, I. A. Medina Rodriguez, S. He, W. Bitter, B. Ewa Snaar-Jagalska, and H. P. Spaink. 2004. Expression analysis of the Toll-like receptor and TIR domain adaptor families of zebrafish. *Mol. Immunol.* 40: 773–783.
31. Yilmaz, A., S. Shen, D. L. Adelson, S. Xavier, and J. J. Zhu. 2005. Identification and sequence analysis of chicken Toll-like receptors. *Immunogenetics* 56: 743–753.
32. Latz, E., A. Schoenemeyer, A. Visintin, K. A. Fitzgerald, B. G. Monks, C. F. Knetter, E. Lien, N. J. Nilsen, T. Espevik, and D. T. Golenbock. 2004. TLR9 signals after translocating from the ER to CpG DNA in the lysosome. *Nat. Imnunol.* 5: 190–198.
33. Tsujita, T., H. Tsukada, M. Nakao, H. Oshiumi, M. Matsumoto, and T. Seya. 2004. Sensing bacterial flagellin by membrane and soluble orthologs of Toll-like receptor 5 in rainbow trout (*Onchorhynchus mikiss*). *J. Biol. Chem.* 279: 487588–48597.
34. Fukui, A., N, Inoue, M. Matsumoto, M. Nomura, Y., Matsuda, K. Toyoshima, and T. Seya. 2001. Molecular cloning and functional characterization of chicken Toll-like receptors. *J. Biol. Chem.* 276: 47143–47149.
35. Takeda, K., O. Takeuchi, and S. Akira. 2002. Recognition of lipopeptides by Toll-like receptors. *J. Endotoxin Res.* 8: 459–463.
36. Ozinsky, A., D. M. Underhill, J. D. Fontenot, A. M. Hajjar, K. D. Smith, C. B. Wilson, L. Schroeder, and A. Aderem. 2000. The repertoire for pattern recognition of pathogens by the innate immune system is defined by cooperation between Toll-like receptors. *Proc. Natl. Acad. Sci. USA* 97: 13766–13771.
37. Couillault, C., N. Pujol, J. Reboul, L. Sabatier, J. F. Guichou, Y. Kohara, and J. J. Ewbank. 2004. TLR-independent control of innate immunity in *Caenorhabditis elegans* by the TIR domain adaptor protein TIR-1, an ortholog of human SARM. *Nat. Imnunol.* 5: 488–494.
38. Finstad, J., and R. A. Good. 1964. The evolution of the immune response. III. Immunologic responses in the lamprey. *J. Exp. Med.* 120: 1151–1168.
39. Nonaka, M., T. Fujii, T. Kaidoh, S. Natsuume-Sakai, M. Nonaka, N. Yamaguchi, and M. Takahashi. 1984. Purification of a lamprey complement protein homologous to the third component of the mammalian complement system. *J. Immunol.* 133: 3242–3249.
40. Nonaka, M., and M. Takahashi. 1992. Complete complementary DNA sequence of the third component of complement of lamprey. Implication for the evolution of thioester containing proteins. *J. Inununol.* 148: 3290–3295.
41. Schluter, S. F., J. Schroeder, E. Wang, and J. J. Marchalonis. 1994. Recognition molecules and immunoglobulin domains in invertebrates. *Ann. NY Acad. Sci.* 712: 74–81.
42. Azumi, K., R. De Santis, A. De Tomaso, I. Rigoutsos, F. Yoshizaki, M. R. Pinto, R. Marino, K. Shida, M. Ikeda, M. Ikeda, et al. 2003. Genomic analysis of immunity in a Urochordate and the emergence of the vertebrate immune system. *Immunogenetics* 55: 570–581.

Wild-Type Measles Virus Infection in Human CD46/CD150-Transgenic Mice: CD11c-Positive Dendritic Cells Establish Systemic Viral Infection[1]

Masashi Shingai,[2*†] Naokazu Inoue,[2‡] Tsuyoshi Okuno,[‡] Masaru Okabe,[‡] Takashi Akazawa,[*] Yasuhide Miyamoto,[*] Minoru Ayata,[§] Kenya Honda,[¶] Mitsue Kurita-Taniguchi,[*] Misako Matsumoto,[*†] Hisashi Ogura,[§] Tadatsugu Taniguchi,[¶] and Tsukasa Seya[3†]

We generated transgenic (TG) mice that constitutively express human CD46 (huCD46) and/or TLR-inducible CD150 (huCD150), which serve as receptors for measles virus (MV). These mice were used to study the spreading and pathogenicity of GFP-expressing or intact laboratory-adapted Edmonston and wild-type Ichinose (IC) strains of MV. Irrespective of the route of administration, neither type of MV was pathogenic to these TG mice. However, in ex vivo, limited replication of IC was observed in the spleen lymphocytes from huCD46/huCD150 TG and huCD150 TG, but not in huCD46 TG and non-TG mice. In huCD150-positive TG mouse cells, CD11c-positive bone marrow-derived myeloid dendritic cells (mDC) participated in MV-mediated type I IFN induction. The level and induction profile of IFN-β was higher in mDC than the profile of IFN-α. Wild-type IC induced markedly high levels of IFN-β compared with Edmonston in mDC, as opposed to human dendritic cells. We then generated huCD46/huCD150 TG mice with type I IFN receptor (IFNAR1)$^{-/-}$ mice. MV-bearing mDCs spreading to draining lymph nodes were clearly observed in these triple mutant mice in vivo by i.p. MV injection. Infectious lymph nodes were also detected in the double TG mice into which MV-infected CD11c-positive mDCs were i.v. transferred. This finding suggests that in the double TG mouse model mDCs once infected facilitate systemic MV spreading and infection, which depend on mDC MV permissiveness determined by the level of type I IFN generated via IFNAR1. Although these results may not simply reflect human MV infection, the huCD150/huCD46 TG mice may serve as a useful model for the analysis of MV-dependent modulation of mDC response. *The Journal of Immunology,* **2005, 175: 3252–3261.**

Measles virus (MV)[4] causes severe immune suppression followed by secondary infections that result in high rates of mortality of infants particularly in developing countries. Human CD46 (huCD46) (1, 2) and TLR-inducible human CD150 (huCD150) (3, 4) have been identified as MV receptors. Although huCD150 is the primary entry receptor for MV, it is not expressed in epithelial cells of the respiratory tract through which MV infection is known to initiate. The mechanism of wild-type MV spreading to systemic organs, therefore, remains unsolved.

No entry receptor for MV has been identified in mice. MV tropism is represented by its receptors, huCD46 and huCD150. Although rodents express the orthologues of these receptors, they fail to act as entry receptors for MV (2, 5, 6). MV infection of adult rodents is restricted to the brain-adapted strains obtained by intracerebral inoculations (7, 8). Transgenic (TG) mice expressing either huCD46 (9–11) or huCD150 (12, 13) have been established as models to investigate MV pathogenicity. Initially, most of the studies were performed using huCD46 TG mice. MV entry was found to be more efficient in mouse cells that express huCD46, the receptor for the MV vaccine Edmonston (ED) strain (1), and probably for several wild-type strains as well (14). However, TG rodents expressing huCD46 are not susceptible to MV infection when inoculated by routes other than intracerebral injection (15). Depletion of type I IFN receptors in the huCD46 TG mice led to high susceptibility to ED (16–18). These earlier studies, however, were performed before huCD150 was identified as the main receptor for wild-type MV strains (4). No in vivo studies have been attempted using wild-type MV strains and huCD46/huCD150 double TG mice for understanding the mechanisms of wild-type MV infection.

Using huCD150 single TG mice, several reports (12, 13) suggested that wild-type MV strains infect cells that constitutively express huCD150 but fail to induce systemic infection. huCD150 is inducible in human T cells and is up-regulated in myeloid dendritic cells (mDCs) and B cells in response to activation signaling from TLR (19–21). Thus, TG construct with just *lck* or CD11c

*Department of Immunology, Osaka Medical Center for Cancer and Cardiovascular Diseases, Osaka, Japan; †Department of Microbiology and Immunology, Graduate School of Medicine, Hokkaido University, Sapporo, Japan; ‡Genome Information Research Center, Osaka University, Suita, Osaka, Japan; §Department of Virology, Osaka City University Medical School, Osaka, Japan; and ¶Department of Immunology, Graduate School of Medicine and Faculty of Medicine, University of Tokyo, Tokyo, Japan

Received for publication February 4, 2005. Accepted for publication June 15, 2005.

The costs of publication of this article were defrayed in part by the payment of page charges. This article must therefore be hereby marked *advertisement* in accordance with 18 U.S.C. Section 1734 solely to indicate this fact.

[1] This work was supported in part by the Core Research for Evolutional Science and Technology (CREST), Japan Science and Technology Agency, by grants-in-aid from the Ministry of Education, Science, and Culture (Specified Project for Advanced Research), by the Ministry of Health and Welfare of Japan, the Naito Memorial Foundation (to M.M.), and by the Grant 11444 for graduate students from the Ministry of Education, Science, and Culture (to N.I.).

[2] M.S. and N.I. equally contributed to this work.

[3] Address correspondence and reprint requests to Dr. Tsukasa Seya, Department of Microbiology and Immunology, Graduate School of Medicine, Hokkaido University, Kita-ku, Sapporo 060-8637, Japan. E-mail address: seya-tu@med.hokudai.ac.jp

[4] Abbreviations used in this paper: MV, measles virus; BAC, bacterial artificial chromosome; CHO, Chinese hamster ovary; CYT, cytoplasmic tail; DC, dendritic cell; mDC, myeloid DC; pDC, plasmacytoid DC; ED, Edmonston; IC, Ichinose; IFNAR1, type I IFN-$\alpha\beta$ receptor; MALP, macrophage-activating lipopeptide; TG, transgenic; EGFP, enhanced GFP; MOI, multiplicity of infection; $TCID_{50}$, 50% tissue culture infective dose; IRF, IFN regulatory factor; CYT, cytoplasmic tail.

0022-1767/05/$02.00

promoter reported earlier (12, 13) may not be adequate for the study of natural huCD150 distribution, MV entry, and resultant infection via huCD150. Establishment of huCD46/huCD150 double TG mice with human-like distribution profile are necessary for the analysis of wild-type MV spreading and following host immunomodulatory events, particularly measles-mediated immune suppression (22–24).

Therefore, for this study, we generated huCD46/huCD150 double TG mice with or without type I IFN-$\alpha\beta$ receptor (IFNAR1). MV replication and spreading were surveyed by GFP-expressing wild-type Ichinose (IC) strain. In in vivo infection studies, however, neither type of MV was pathogenic to these TG mice irrespective of the route of administration. Analyses of these TG mice suggested that the critical factor in wild-type MV systemic infection appears to depend on the level of type I IFN generated by CD11c-positive dendritic cells (DCs) in this mouse model. In fact, DCs were infected with MV in the huCD150-positive TG mice with no IFNAR1. In this study, we first report that huCD46/huCD150 double TG mice are sensitive to wild-type MV once MV-infected mDCs are supplemented. Thus, infected mDCs facilitate establishing systemic MV infection in the TG mice. These double TG mice allow us to analyze immunomodulatory function of the MV receptors during MV infection (25, 26). The double TG mice with human-like huCD46/huCD150 expression profiles may be a better model for wild-type MV infection compared with huCD150 constitutively expressing mice.

Materials and Methods

Cell culture and reagents

Vero, Vero/huCD150 (a signaling lymphocyte activation molecule (SLAM)), which are Vero cells with stable expression of huCD150 obtained by transfection of huCD150/pCXN2 and antibiotic selection, HEK293, and 293-3-46 cells, kindly provided by M. A. Billeter (Institute of Molecular Biology, University of Zurich, Zurich, Switzerland) were maintained in DMEM supplemented with 10% heat-inactivated FCS and antibiotics. B95a cells were maintained in RPMI 1640 supplemented with 5% heat-inactivated FCS (JRH Biosciences) and antibiotics. Polymyxin B, LPS from *Escherichia coli* serotype O111:B4 was from Sigma-Aldrich. The mycoplasma lipopeptide macrophage-activating lipopeptide (MALP)-2 was prepared as described (27). MALP-2 was treated with polymyxin B (10 μg/ml) for 1 h at 37°C before stimulation of cells (27). Usually, 100 ng/ml LPS and 100 nM MALP-2 were used in mDC TLR stimulation. Isotype controls for PE rat IgG2a, PE rat IgG2b, PE mouse IgG1, PE or FITC golden syrian hamster IgG, FITC mouse IgG1, and FITC mouse IgG2a, and mAbs for PE anti-mouse CD8a, PE anti-mouse CD4, PE anti-mouse CD3e, PE anti-mouse CD19, PE anti-human CD3e, PE anti-human CD4, PE anti-human CD8a, PE anti-human CD19, and FITC anti-huCD150 were obtained from eBioscience. FITC or PE anti-mouse CD11c mAb was obtained from BD Pharmingen. FITC anti-huCD46 (MCP) mAb was obtained from Ancell. HRP-conjugated goat anti-rabbit Igs were obtained from American Qualex. Rabbit polyclonal bodies against huCD150 or huCD46 were produced in our laboratory.

TG method

Spermatozoa were dispersed from epididymis of 12-wk-old mature B6D2F$_1$ male mice in 400 μl of TYH medium diluted to 1 × 10^7/ml and frozen in liquid nitrogen immediately. The bacterial artificial chromosome (BAC) DNA carrying huCD46 or huCD150 was purchased from Incyte Genomics, and purified by using Large-Construct kit (Qiagen) according to the manufacturer's instructions. Each BAC DNA (5 μg/ml in TE buffer) was added to the thawed sperm. The mixtures were incubated for 5 min at room temperature, and mixed with one-tenth volume of 12% PVP-HCZB (polyvinyl-pyrrolidone-HEPES-Chatot, Ziamok, and Barister medium). The metaphase II oocytes for microinjection from B6D2F$_1$ female mice were prepared as previously described (28). These oocytes were maintained in kSOM (potassium simplex optimized medium) under mineral oil equilibrated in 5% (v/v) CO_2 in air at 37°C until use.

Generation of huCD46 and huCD150 TG mice

The huCD46 and huCD150 TG mice were produced by using the intracytoplasmic sperm injection transgene method (29). TG mice were made in accordance of the guidelines of the Animal Care and Use Committee of Osaka University. For microinjection, sperm heads were aspirated into a pipette attached to a piezoelectric pipette-driving unit and a sperm head was injected into each oocyte as previously described (28). After injection, the eggs were incubated in kSOM to the 2-cell stage, and were transferred to ICR pseudopregnant females. Among pups born, the huCD46 and huCD150 TG mice were detected by genomic PCR using huCD46- and huCD150-specific primers. The PCR primers used were as follows: 5′-AAAGGGCAAATTACCTTAGGGGTG-3′ and 5′-AGCACTTCGACC TAAAAATAGAGAT-3′ for huCD46 and 5′-GTGATACAGGAAGCG GGTTCAGG-3′, and 5′-GATACGCTGATTCCTGGCAGCTAAC-3′ for huCD150.

Southern blotting was performed with PCR products from human genome using those primers and with DIG High Prime DNA Labeling and Detection starter kit II (Roche Applied Science).

The IFNAR1$^{-/-}$ mouse (30) was obtained from The Jackson Laboratory. All mice were backcrossed at least six times to be a C57/BL6J background.

Western blotting

Various tissues from huCD46 and huCD150 TG mice were homogenized by a Potter-type homogenizer in 1% (v/v) Triton X-100, PBS, 1 mM PMSF, 10 mM benzamidine, 1 μg/ml pepstatin, and 1 μg/ml lepeptin. The extracts were centrifuged at 15,000 × g, and protein was estimated by Bio-Rad color reagent. A total of 20 μg of protein was subjected to SDS-PAGE under nonreducing conditions and transblotted onto nylon membranes. The membranes were incubated with anti-huCD46 polyclonal Ab or anti-huCD150 polyclonal Ab for 2 h, washed with PBS containing 0.5% Tween 20 three times and incubated with HRP-conjugated goat anti-rabbit Igs for 1 h at 37°C. Following second incubation, the membranes were washed three times with PBS-Tween 20 and proteins were detected with an ECL chemiluminescence kit (Amersham Biosciences).

Plasmid construction and rescue of recombinant viruses

For the preparation of wild-type MV IC-B strain (31, 32) expressing enhanced GFP (EGFP), we constructed p(+)MV323/GFP. Fragment 1, which has *Bss*HII site T7 promoter leader sequence with *Eco*RI site, was amplified by PCR with p(+)MV323/GFP as template using forward primer 5′-AGTCCGCGGGAgcgcgcGTAATACGACTCACTA-3′ (gcgcgc is *Bss*HII site and underline is T7 promoter), and reverse primer 5′-CG gaattcTCCCTAATCCTGCTCTTGTCCC-3′ (gaattc is *Eco*RI site and underline is a part of 5′ noncoding region of the N gene). Fragment 2, which has *Not*I site, the N gene terminator gene junction front half of the N gene with *Hin*dIII site, was amplified by PCR using p(+)MV323/GFP as template with forward primer 5′-CTgcggccgcATTGTTATAAAAAACTTAGG ATTCAAGATCCTATTA-3′ (gcggccgc is *Not*I site and underline is the N gene terminator, gene junction, and the N gene initiator) and reverse primer CCCaagcttCCTCTCGCACCTAGTCTAGAAGAT-3′ (aagctt is *Hin*dIII site and underline is a part of N gene coding region). The fragment 1 was digested with *Bss*HII and *Eco*RI, fragment 2 was digested with *Not*I and *Hin*dIII, and the EGFP gene was cut from pEGFP-N1 plasmid (Clontech Laboratories) with *Eco*RI and *Not*I. These three DNA fragments were ligated and the chimeric plasmid clone containing 5′ *Bss*HII site, T7 promoter, leader initiation signal (the 5′ region of the N gene) EGFP gene, and junction (a termination sequence of the 3′ region of the N gene/CTT sequence (the 5′ region of the N gene containing an initiation sequence), which have *Esp*I site) 3′ sequences, was generated. The accuracy of the fragment was confirmed by sequencing. The insert and p(+)MV323 were digested with *Bss*HII and *Esp*I, and the fragment containing an EGFP gene was inserted into p(+)MV323.

Recovery of infectious MV was performed as previously described (33, 34). MV323, MV323/GFP, and MV2A (ED strain) were recovered from p(+)MV323, p(+)MV323/GFP, and p(+)MV2A, respectively.

Immunofluorescence staining and confocal microscopy

Mock- or MV323GFP-infected mouse splenocytes were stained with PE rat IgG2a isotype control, PE rat IgG2b isotype control, PE golden syrian hamster IgG isotype control, PE anti-mouse CD8a mAb, PE anti-mouse CD4 mAb, PE anti-mouse CD3e mAb or PE anti-mouse CD19 mAb for 30 min at 4°C in FACS buffer. After washing, the stained cells were fixed in 0.5% formaldehyde in PBS and visualized at a magnification ×60 under a FLUOVIEW (Olympus). Images were captured using the attached computer FLUOVIEW software.

FACS cytometric analysis of cell surface Ags

FACS methods were previously described (35). Briefly, cells were suspended in PBS containing 0.1% sodium azide and 1% BSA (FACS buffer) and incubated for 30 min at 4°C with FITC-labeled mAbs and PE-labeled mAbs. Cells were washed and fluorescence intensity was measured by FACS.

Preparation of MV strains and in vitro MV infection analysis

Recovered viruses, MV2A (ED strain), MV323 (IC-B strain), and MV323GFP (IC-B strain containing EGFP gene), were passaged in B95a cells and titrated on Vero/SLAM cells. Low-passaged viruses were used in this experiment. The receptor usage of the strains was confirmed on Chinese hamster ovary (CHO), CHO/huCD46, or CHO/huCD150 cells (5). For in vitro viral infection assay, single cell suspensions of spleen from TG or non-TG littermates were obtained by passage thought sterile mesh. After removing erythrocytes using Lympholyte-M (Cedarlane Laboratories), purified cells were cultured in RPMI 1640 supplemented with 10% heat-inactivated FCS, 10 mM HEPES, 1 mM sodium pyruvate, 0.1 mM nonessential amino acids, 0.05 mM 2-ME, 50 U/ml mouse IL-2, 20 ng/ml PMA, and 1 μg/ml ionomycin for 24 h. FACS analysis was performed 48 h after infection.

Preparation of DCs

Mouse bone marrow-derived mDCs were prepared by the modified technique (36, 37) of earlier reported method (38). Briefly, 0.5–1 × 10^6 bone marrow cells/2 ml/well in RPMI 1640 supplemented with 10% heat-inactivated FCS, 10 mM HEPES, 1 mM sodium pyruvate, 0.1 mM nonessential amino acids, and 0.05 mM 2-ME were cultured overnight in 24-well plates. Nonadherent cells were harvested, resuspended in the same medium supplemented with 10 μg/ml mouse GM-CSF, and cultured in the mouse GM-CSF-containing medium. On day 3, adherent cells were cultured in fresh medium with 10 μg/ml mouse GM-CSF. On day 6, nonadherent cells and loosely adherent cells were harvested and used for experiments as immature DCs (38). Immature DCs were resuspended and cultured in fresh RPMI 1640 medium with 10 μg/ml mouse GM-CSF. Cellular RNA was estimated 24 h postinfection.

Human PBMC were isolated from buffy coat of normal healthy donors by methylcellulose sedimentation followed by standard density gradient centrifugation with Ficoll-Hypaque (Amersham Biosciences) (27). For human immature DC preparation, $CD14^+$ monocytes were obtained from human PBMC by using MACS system (Miltenyi Biotec) with anti-human CD14 mAb-conjugated microbeads and kept in RPMI 1640 (Invitrogen Life Technologies) containing 10% FCS, 500 IU/ml human GM-CSF, 100 IU/ml human IL-4 (PeproTech), and antibiotics for 6 days. Morphological changes were examined by phase contrast microscopy (Olympus IX-70).

Assay of in vivo MV infection

Newborn 2-day-old, 1-wk-old, or 6- to 10-wk-old TG or non-TG mice were injected i.p., i.v., intranasally, and s.c. with MV323GFP at a dose of 5 × 10^4 50% tissue culture infective doses ($TCID_{50}$). Mice were sacrificed 2–4 days after inoculation, and each tissue was collected and fixed with 4% paraformaldehyde in PBS overnight at 4°C. Tissues were embedded in Tissue-Tek OCT compound (Miles) and quickly frozen in liquid nitrogen. Serial frozen sections (10-μm thick) were cut with the cryostat (Leica) and were analyzed by confocal microscopy.

In vitro splenocytes proliferation assay

Splenocytes (1 × 10^5/100 μl/well in 96-well plate) freshly isolated from each TG mouse were stimulated with 20 ng/ml PMA and 1 μg/ml ionomycin in the presence of 50 U/ml mouse IL-2, and infected by MV323. Twenty-four hours later the cells were labeled for 16 h with [^{3}H]thymidine (1 mCi/ml). The incorporated counts were determined using a beta-plate reader in triplicate.

RT-PCR and quantitative PCR

Mouse mDCs or splenocytes were treated with trypsin and collected by centrifugation at 1500 × *g* for 10 min. Total RNA was extracted with RNeasy mini kit (Qiagen). A total of 2 μg of total RNA was incubated at 70°C for 5 min, kept on ice for 2 min, and reverse transcription was performed with Moloney murine leukemia virus-reverse transcriptase (Promega) at 37°C for 90 min followed by PCR or quantitative PCR. Following primers were used for PCR: α-IFN forward, 5′-AGTGATGAGCTAC TGGTCAAC-3′; reverse, 5′-TGATGCTGTGGAAGTATATCCTC-3′; β-IFN forward, 5′-TCCAGCTCCAAGAAAGGACG-3′; reverse, 5′-GCATCTTCTCCGTCATCTCC-3′; γ-IFN forward, 5′-AGACAGAAGT TCTGGGCTTCTC-3′; reverse, 5′-GGGTTGTTGACCTCAAACTTGG-3′; MV-H forward, 5′-CCCTTATCAACGGATGATCC-3′; reverse, 5′-GT GATCAATGGCCCGAATCC-3′; MV-N forward, 5′-AAGGTCAGTTC CACATT-3′; reverse, 5′-GAAGATCTCTGTCATTG-3′; IL-12 p40 forward, 5′-GAGTCATAGGCTCTGGAAAGACC-3′; reverse, 5′-AGTT GGGCAGGTGACATCC-3′; IL-10 forward, 5′-GGTTGCCAAGCCT TATCGGA-3′; reverse, 5′-ACCTGCTCCACTGCCTTGCT-3′; β-actin forward, 5′-ATCATGTTTGAGACCTTCAACACC-3′; reverse, 5′-GAT GTCACGCACGATTTCCC-3′; and HPRT (hypoxanthine phosphoribosyltransferase) forward, 5′-GTTGGATACAGGCCAGACTTTGTTG-3′, reverse, 5′-GAAGGGTAGGCTGGCCTATAGGCT-3′.

Reaction for quantitative PCR was done with iQ SYBER Green Supermix, and amplified PCR products were measured by iCycler iQ Real-Time PCR analyzing system (Bio-Rad). Normalized value for each mRNA expression was calculated as relative quantity of mRNA divided by the relative quantity of mouse hypoxanthine phosphoribosyltransferase.

Determination of human IFN-β level

Culture media were centrifuged to remove cell debris and supernatants were stored at −80°C until the assay. The level of secreted human IFN-β in the culture medium was determined with an ELISA kit (FUJIREBIO) for human IFN-β according to the manufacturer's protocol.

Results

Human-like expression of huCD46 or huCD150 in TG mice

Ubiquitous expression of huCD46 was not obtained in TG mice that were previously generated with huCD46 cDNA (39). A number of splicing variants in huCD46, which appeared in an organ-specific manner (40), participated in differential cell-mediated immune response (26). To generate the natural expression profile of huCD46 and its isoforms, we transferred the 194-kb BAC DNA carrying the huCD46 gene into mouse embryo and obtained TG mice with human-like CD46 expression pattern. Similarly, huCD150 TG mice were generated by transferring the huCD150 BAC DNA (185 kb) into mouse embryo. These mice have a human-like CD150 expression profile, which is inducible in T cells and up-regulated in mDCs and B cells. We examined the expression profiles of huCD46 and huCD150 in various organs of each line of our TG mice by SDS-PAGE and Western blotting (Fig. 1*A*). In huCD46 TG mice, huCD46 was ubiquitously expressed with the size variation of isoforms in an organ-specific fashion similar to human (41, 42). The brain of these mice notably expressed a low molecular mass moiety of huCD46 in the TG mice similar to human form. In addition, similar to human, huCD150 appeared in a tissue-specific manner in the thymus and spleen in huCD150 TG mice. In non-TG mice, no signals of huCD46 or huCD150 were detected in Western blots, suggesting no cross-reaction of the Abs with the mouse counterparts.

Cell populations expressing huCD46 or huCD150 in TG mice

We next analyzed cells from spleens of huCD46 TG, huCD150 TG, or non-TG mice by FACS analysis (Fig. 1*B*). In huCD46 TG mice, huCD46 was expressed on the surface of both CD3- or CD19-positive splenocytes. In huCD150 TG mice, huCD150 was expressed on CD19-positive cell surface, but minimal expression occurred on CD3-positive cells. Neither CD4 nor CD8 T cells expressed huCD150 (data not shown). Under similar FACS conditions, human PBMC ubiquitously expressed CD46 and partly expressed CD150 (Fig. 1*B*, *right*). When splenocytes from huCD150 TG mice were stimulated with PHA (data not shown) or PMA, ionomycin, and murine IL-2 (Fig. 1*C*, *left*), FACS profiles of the lymphocyte populations were altered. In addition, the levels of huCD150 in $CD4^+$ and $CD8^+$ T cell and $CD19^+$ B cell populations were up-regulated (Fig. 1*C*). Similar results were obtained with human PBMC when the cells were similarly stimulated (Fig. 1*C*, *right*). Neither huCD46 nor huCD150 was expressed in cells from non-TG mice as expected (see Fig. 5, *B* and *C*, labeled as

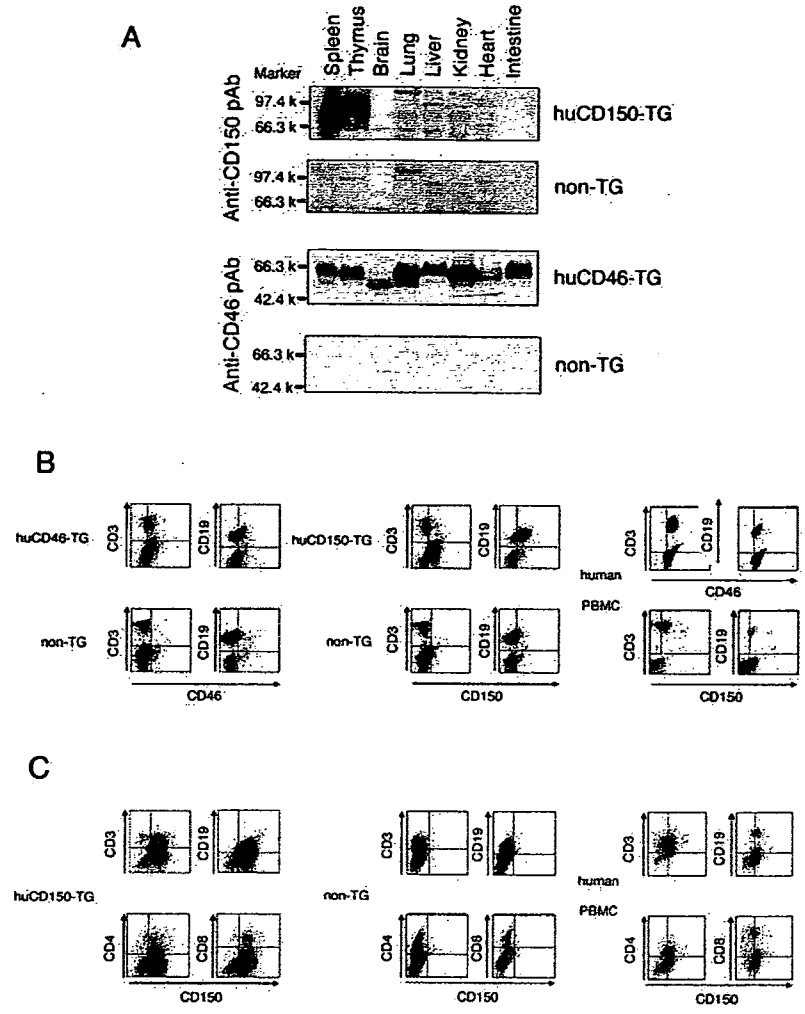

FIGURE 1. Generation of huCD46 and huCD150 TG mice. A, Western blot analysis of huCD46 and huCD150 in TG mice. Various tissues from huCD46 TG and huCD150 TG mice were homogenized and the extracts were separated by SDS-PAGE under nonreducing conditions and transblotted onto a nylon membrane. The huCD46 and huCD150 were then visualized with anti-human CD46 polyclonal Ab and anti-human CD150 polyclonal Ab, respectively, produced in our laboratory (64). *B* and *C*, FACS analysis for detection of huCD46 and huCD150 in mouse spleen cell populations and human PBMC. Freshly isolated splenocytes from the huCD46 and huCD150 TG mice or human PBMC were stained with FITC-labeled anti-human CD46 or CD150 mAb, and PE-labeled mCD3, mCD4, mCD8, or mCD19 mAb before (*B*) or after (*C*) stimulation with PMA and ionomycin.

"non-TG"). These results show that huCD150-inducible TG mice were established, which may suit the study for susceptibility of cell species to MV strains.

We then generated huCD46/huCD150 double TG mice by mating both TG lines (Fig. 2*A*). Gene analysis showed that the littermates of huCD46/huCD150 TG, huCD46 TG, huCD150 TG, and non-TG mice followed Mendel's laws of inheritance (Fig. 2*A*), suggesting that huCD46/huCD150 transgene does not bring about any lethal defect. The presence of huCD46 and huCD150 genes in litters was monitored by PCR (data not shown) and confirmed by Southern blot analysis (Fig. 2*B*). Expression profiles of huCD46 and huCD150 in each litter were also confirmed by Western blot and FACS analysis (data not shown).

Preparation of EGFP-labeled MV

To monitor MV infection, we generated EGFP-expressing recombinant MV (IC323GFP) based on the wild-type IC strain. Plasmid containing full-length cDNA of the IC strain and the EGFP gene was constructed as shown in Fig. 3*A*. GFP expression reflects viral replication in this construct. The rescued MV323GFP showed almost the same growth kinetics as the parental recombinant MV323. Its receptor usage was confirmed with CHO cells expressing huCD46 or huCD150 (Fig. 3*B*). MV2A (ED strain) rescued from p(+)MV2A, was used as the laboratory-adapted strain. When infected with MV2A, both CHO/huCD46 and CHO/huCD150 cells produced the typical syncytia, whereas MV323 infected CHO/huCD150 cells but not CHO/huCD46 cells (data not shown). MV323GFP also infected CHO/huCD150 cells to form syncytia exhibiting green autofluorescence, but did not form any syncytium in CHO/huCD46 and intact CHO cells.

In vitro analysis of MV infection of splenocytes from TG mice

To examine in vitro MV infection, the splenocytes were isolated from each TG mouse and infected with MV323GFP at a multiplicity of infection (MOI) of 0.25 (Fig. 4*A*). When prestimulated with PMA and ionomycin, some splenocytes from the double TG or huCD150 TG mice were positive in GFP, a marker for infection. The stimulation was essential for MV permissiveness as reported before (14). However, under any infectious conditions the splenocytes from huCD46 TG and non-TG mice were GFP-negative. The results were confirmed to be reproducible by semiquantitative FACS analysis (Fig. 4*A*). In contrast, MV323GFP infected human PBMC even at low MOI of inoculation (Fig. 4*A*, *bottom panels*). Human PBMC appear to be more susceptible to MV323GFP than the splenocytes of the double TG and huCD150 TG mice.

To examine which populations of splenocytes of huCD46/huCD150 TG or huCD150 TG mice were infected with MV323GFP, we segregated them with PE-conjugated anti-mouse CD3, CD4, CD8, CD11c, or CD19 mAb and analyzed them by FACS and confocal microscopy (Fig. 4, *B* and *C*). MV323GFP inoculation rendered the CD3-, CD4-, CD8-, and CD19-positive cells green. But CD11c-positive cells barely turned green even at

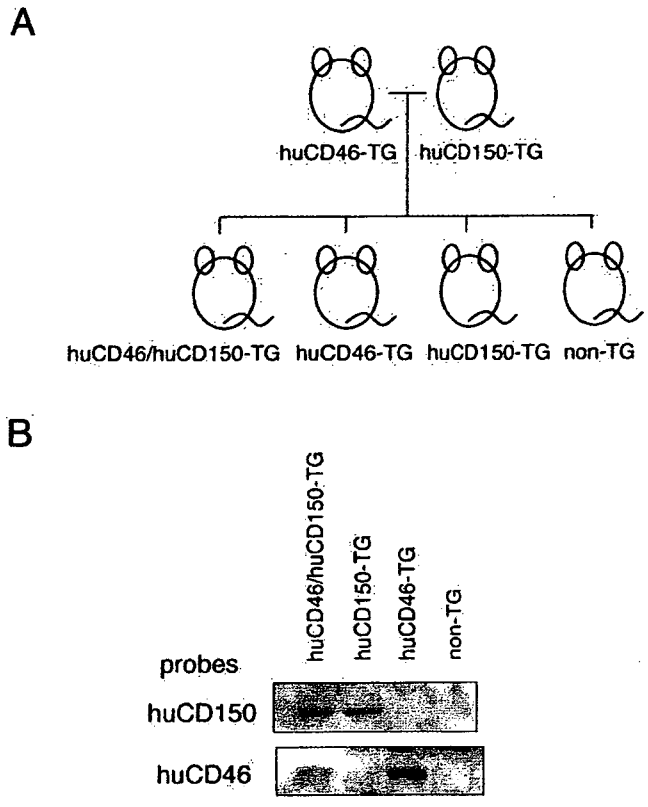

FIGURE 2. Scheme for generation of double TG mice and confirmation of genotypes. *A*, Heterogenic human CD46 and human CD150 TG mice were mated, and Mandelian inheritance of the offspring of huCD46/huCD150, huCD46, huCD150 is diagrammatically represented. *B*, Southern blots of gene transfer profiles of double TG mice.

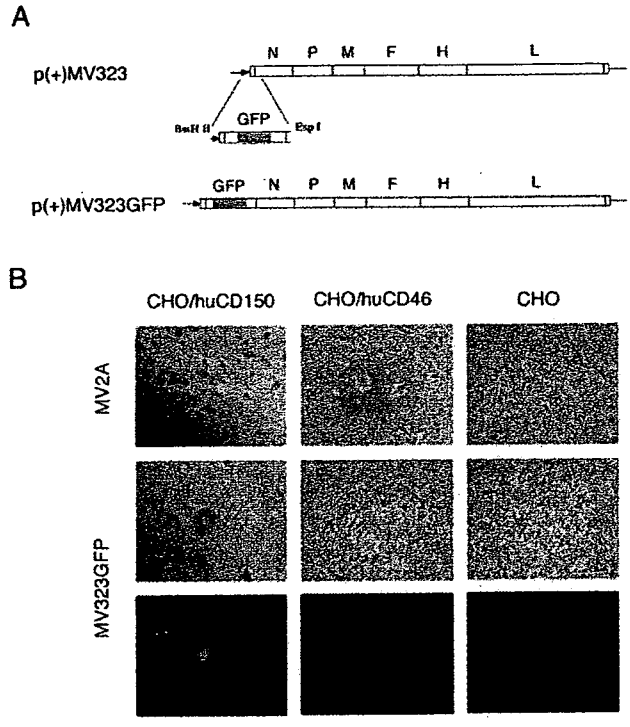

FIGURE 3. Generation of EGFP-labeled wild-type MV (MV323GFP). *A*, Scheme for GFP-labeled MV323 (MV323GFP) construction shows the p(+)MV323 plasmid (*upper*) coding wild-type MV IC strain antigenome and a construct of EGFP. The EGFP construct was placed upstream of the N gene of IC. The construct of p(+)MV323GFP that expresses GFP and viral proteins is also shown (*lower*). *B*, Receptor usage of MV323GFP. Rescued virus MV323GFP from p(+)MV323GFP was inoculated on CHO/huCD150, CHO/huCD46, and intact CHO cells, and 2 days later receptor tropism of MV323GFP was confirmed by syncytium formation and GFP fluorescence. MV2A (ED strain) rescued from p(+)MV2A was used as a control that can use both receptors. Magnification, ×100.

high MOI inoculation (Fig. 4*B*). Thus, the CD11c-positive splenocytes that are representative of DCs are less susceptible to wild-type MV compared with other cell types.

Wild-type MV fails to infect the TG mice in vivo

Next we examined in vivo MV infection. Six- to 10-wk-old double TG, huCD150 TG, huCD46 TG, or non-TG mice were injected i.p., i.v., intranasally, or s.c. with MV323GFP at a dose of 5×10^4 to 1×10^6 $TCID_{50}$. None of the TG mice showed any sign of illness. Two to 4 days after inoculation, the sections of brain, spleen, thymus, lymph nodes, lung, kidney, liver, intestine, and heart from each mouse were examined for GFP-positive cells to monitor infection by MV323GFP. No GFP-positive cells were detected in any tissue. Following i.p. injection of MV323GFP in newborn 2-day-old or 1-wk-old TG or normal mice, no GFP was detected. Intravenously transferred MV323GFP-infected splenocytes to double TG mouse also did not show any GFP-positive lesions (data not shown).

MV fails to effectively replicate in mouse DC

It was reported earlier that huCD150 were minimally expressed in human monocyte-derived DCs and up-regulated by stimulation of TLRs (20). We confirmed the expression and up-regulation of huCD150 in mDCs from huCD46/huCD150 TG mice (Fig. 5*A*). mDCs prepared from the TG mice by conventional method (the purity confirmed by the CD11c marker) expressed both huCD150 and huCD46 with a pattern similar to human monocyte-derived DCs. When mDCs were stimulated with LPS, a ligand of TLR4, expression of huCD150 was up-regulated. Similar huCD150 up-regulation was observed by stimulation with MALP-2, which is a ligand of TLR2. Of note, the level of huCD46 was not influenced in mDC in which TLRs were stimulated.

Because GFP-positive cells reflecting MV323GFP infection were barely detected in CD11c-positive splenocytes (Fig. 4*B*), we examined whether mDCs prepared from TG or non-TG mice were susceptible to MV. The mDCs from each TG mouse line were inoculated with MV323GFP at MOI = 0.25 (Fig. 5*B*). Only a few GFP-positive cells were found in mDCs from the double TG (Fig. 5*B*, left) and huCD150 TG, but not huCD46 TG and non-TG mice (data not shown). The results were compared with human monocyte-derived DCs. At MOI = 0.25 (Fig. 5*B*, *right*), a number of human DCs turned GFP-positive.

We have reported that human DCs were more susceptible to wild-type MV strains than were the laboratory-adapted and vaccine strains (20). The difference was caused by the ability of MV strains to induce type I IFN in DCs (43, 44). Human monocyte-derived DCs were inoculated with MV323, MV2A, or mock viruses at MOI = 1, whereas human IFN-β was actually produced in culture supernatants as measured by ELISA. As expected, human DCs infected with MV323 produced lower levels of IFN-β than did DCs infected with MV2A (Fig. 6*A*). Then, we examined type I IFN levels in culture supernatants of mDCs challenged with wild-type strain MV323. mDCs prepared from each TG mouse line were incubated with the same lots of MV strains at MOI = 1, and mouse IFN-β mRNA levels were measured by quantitative PCR (Fig. 6*B*). When MV323 infected mDCs from huCD46/huCD150

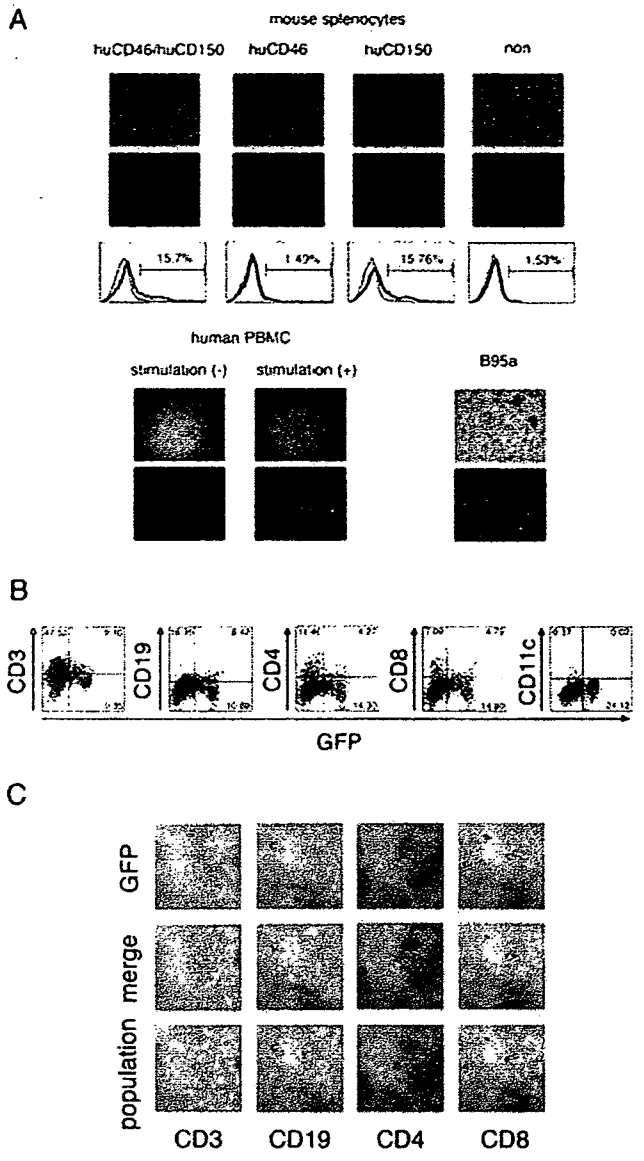

FIGURE 4. In vitro and ex vivo analysis for MV323GFP infection in splenocytes from TG mice. The splenocytes isolated from each TG mouse were stimulated with or without PMA, ionomycin, and, IL-2 and infected with MV323GFP at MOI = 0.25 for 2 days. Cells were observed by fluorescence microscope (*A*), FACS (*B*), and confocal microscope (*C*). *A*, Human PBMC and B95a cells were used as controls. B95a cells were not prestimulated, whereas either stimulated or unstimulated human PBMC and mouse splenocytes were used for infection studies. Magnification, ×40. Infectivity of splenocytes from the indicated mouse line was measured by FACS analysis (*bottom*). Fluorescence intensity reflects the levels of the MV-associated GFP. *B*, Positive cell populations (*inset*) are shown as a percentage. *C*, GFP (infected cells; green) are indicated (*upper*) and the splenocyte populations (CDs, red) are indicated (*lower*). Their merging profiles (yellow) are also shown (*middle*). Magnification, ×200.

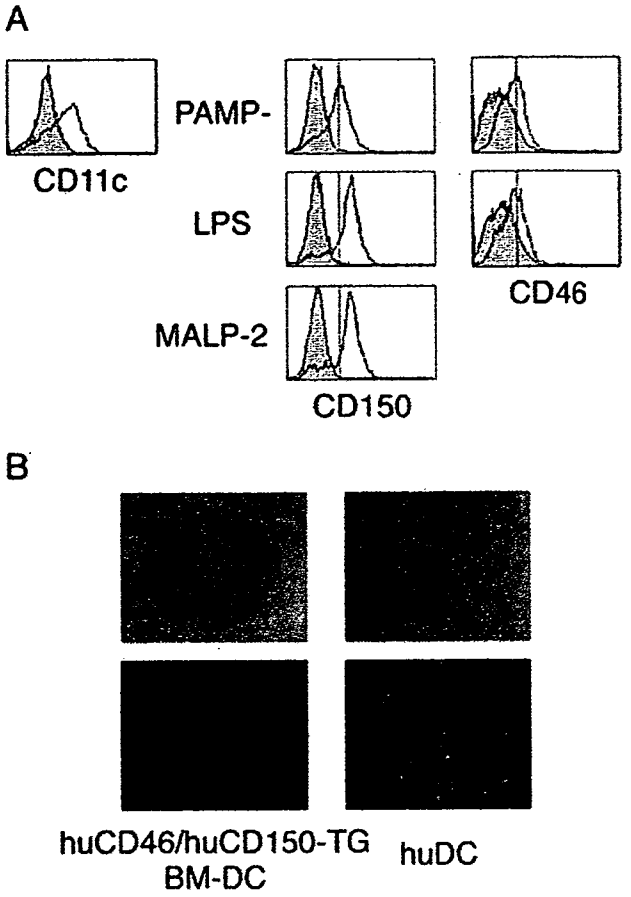

FIGURE 5. Expression profiles of huCD46 and huCD150 and testing MV sensitivity of mDCs. *A*, huCD46 and huCD150 on CD11c-positive mDCs. The expression of CD11c, huCD46, and huCD150 in mDCs prepared from huCD46/huCD150 TG mice were examined using FACS. TLR4 agonist (LPS) and TLR2 agonist (MALP-2) were used as mDC maturation inducers. Control mDCs (PAMP−) were cultured without any TLR stimulator. *B*, Efficacy of MV infection in human monocyte-derived DCs and mDC prepared from the double TG mice. mDCs from each mouse line and human monocyte-derived DCs were infected with MV323GFP at MOI = 0.25. Two days later, cells were observed under fluorescence microscope. Magnification, ×40.

TG and huCD150 TG, the mRNA levels of type-I IFN (IFN-α and IFN-β) were markedly increased in the mDCs (Fig. 6, *B* and *C*). MV2A induced IFN-α and IFN-β in the mDCs from double TG, huCD150 TG, and huCD46 TG (Fig. 6, *B* and *C*). Induction of IFN-α was less compared with IFN-β. In mouse blood cells, however, neither IFN-β nor IFN-α message was virtually detected: only a trace amount of IFN-γ message was measurable (data not shown). Local, rather than systemic, induction of type I IFN-β would occur by mDCs in response to wild-type MV. The levels of total IFN-β production depend on the combined actions of MV strain types and IFN inducibility of mDCs. Because IL-12 p40 and IL-10 were induced from human DCs as a consequence of MV infection, we also measured the mRNA level of murine IL-12 p40 and murine IL-10 of mDCs (Fig. 6, *D* and *E*). Results showed that the mRNAs of these cytokines were also induced by MV infection via the MV receptors. MV infection was confirmed by determination of the mRNA level of the H protein gene of MV (Fig. 6*F*). Although the same lots of virus stocks were used for infection, MV323 replicated better in mDCs from huCD150 TG than huCD46/huCD150 TG mouse lines. MV2A replication was high in mDCs from huCD150 TG and low in mDCs from the double TG and huCD46 TG mouse lines. The coexpressed huCD46 would probably inhibit viral replication in mouse mDCs.

DC have critical role in the establishment of MV infection in vivo

Differential susceptibility to MV of mDCs prepared from huCD46/huCD150 TG mouse vs human DCs earlier described, allowed us to speculate that DCs play a critical role in the development of systemic MV infection in vivo. Because type I IFN induced by

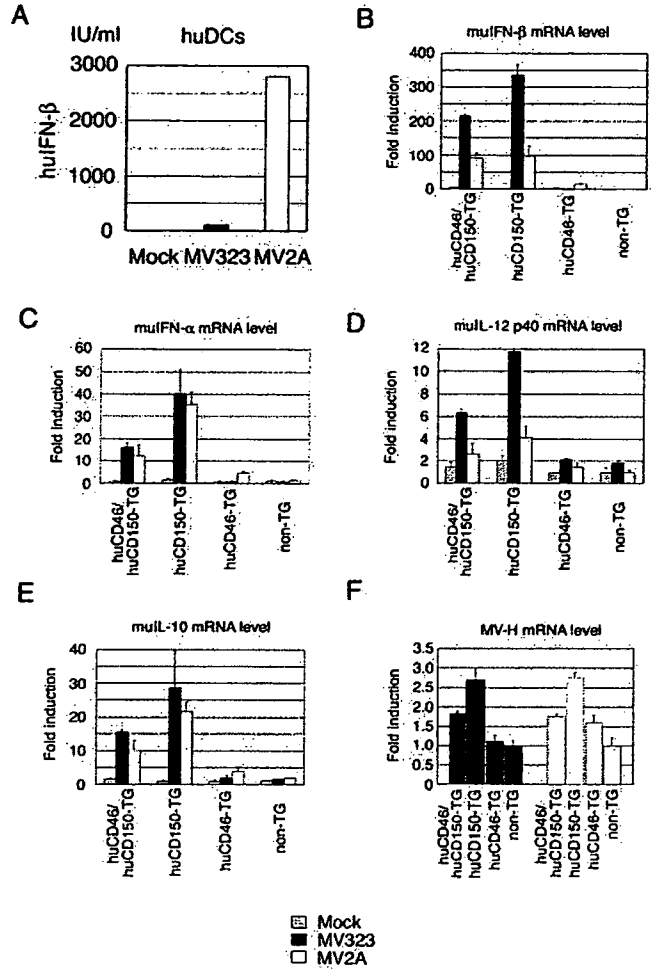

FIGURE 6. MV-induced molecules and cytokines in mouse bone-marrow-derived mDCs. Cytokine induction and MV replication profiles in mDCs prepared from TG mouse lines. *A*, Human monocyte-derived DCs were infected with MV323 or MV2A at MOI = 1. At 24 h after infection the levels of human IFN-β in the supernatants were measured using ELISA. *B*, mDCs were prepared from each indicated TG mouse line and infected with MV323 or MV2A at MOI = 1. At 24 h after infection, the mRNA levels of mouse IFN-β affected by infection with MV323 or MV2A in mDCs were measured by quantitative PCR. Fold induction against mock infection in non-TG is shown. *C–F*, mDCs prepared as in *A* and *B* were similarly infected with MV323 or MV2A at MOI = 1. At 24 h after infection, the mRNA levels of mouse (mu) IFN-α (*C*), IL-12 p40 (*D*), IL-10 (*E*), and MV-H (*F*) were measured by quantitative PCR. Relative fold induction against mock infection in non-TG is shown. The experiments were performed at least three times and represented results are shown.

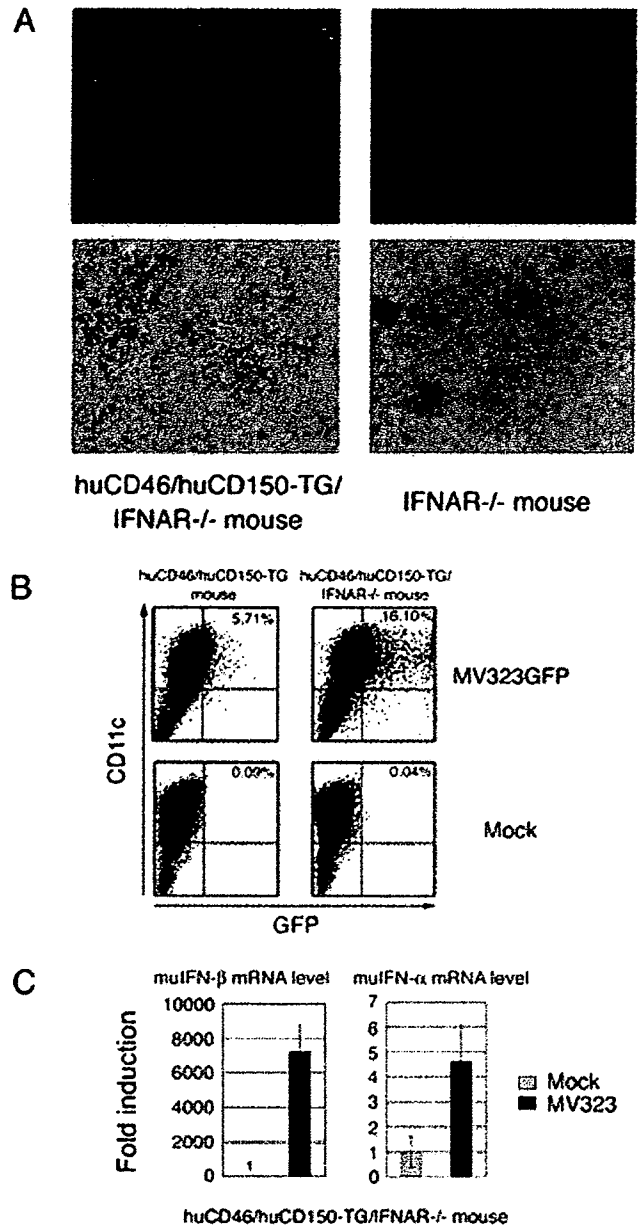

FIGURE 7. mDCs from huCD46/huCD150 TG/IFNAR$^{-/-}$ mice are susceptible against MV infection. *A*, mDCs susceptible to MV. mDCs prepared from huCD46/huCD150 TG/IFNAR$^{-/-}$ mice or IFNAR$^{-/-}$ mice (control) were inoculated with MV323GFP at MOI = 0.25. At 24 h later, cells were observed under fluorescence microscope. Magnification, ×40. *B*, mDCs from huCD46/huCD150 TG and huCD46/huCD150 TG/IFNAR$^{-/-}$ mouse prepared as in *A* were infected with MV323GFP at MOI = 0.25. At 24 h later, cells were stained with PE-labeled mouse CD11c and measured by FACS analysis. *C*, mDCs prepared as in *A* were infected with mock or MV323GFP for 24 h at MOI = 1. The mRNA levels of mouse IFN-β and IFN-α were measured by quantitative PCR. Relative fold induction against mock infection is shown.

wild-type MV acted on huCD46/huCD150-positive mDCs in a positive feedback manner, we generated huCD150/huCD46/IFNAR1$^{-/-}$ triple mutant mice, by mating the double TG mice with the IFN $\alpha\beta$ receptor 1 (IFNAR1) knockout mouse. First, we examined whether mDCs from huCD150/huCD46/IFNAR1$^{-/-}$ mutant mice were susceptible to wild-type MV infection in vitro. When the mDCs were inoculated with MV323GFP at MOI = 0.25, many GFP-positive mDCs were detected by fluorescence microscopy (Fig. 7*A*) and FACS analysis (Fig. 7*B*). Moreover, robust type I IFN production was detected in mDCs (Fig. 7*C*). The mDCs were incubated with MV323 at MOI = 1 for 24 h, and then the mRNA levels of mouse IFN-β and IFN-α were measured using quantitative PCR. As viral replication increased, IFN-β production also increased (Fig. 7, *B* and *C*). IFN-α production was largely suppressed because of the lack of the secondary signal via IFNAR1 (Fig. 7*B*, *right*). Because mDCs in triple mutant mice became susceptible to wild-type MV, we next analyzed the results of in vivo MV infection. For this, the triple mutant mice were injected i.p. with MV323GFP at a dose of 5×10^4 $TCID_{50}$. Two days later, some of the tissues were collected and their sections were directly observed by inverted fluorescence microscope (Fig. 8*A*). GFP-positive cells were detected in mesenteric lymph nodes, inguinal lymph nodes, parathymic lymph nodes, and spleen. Yet,

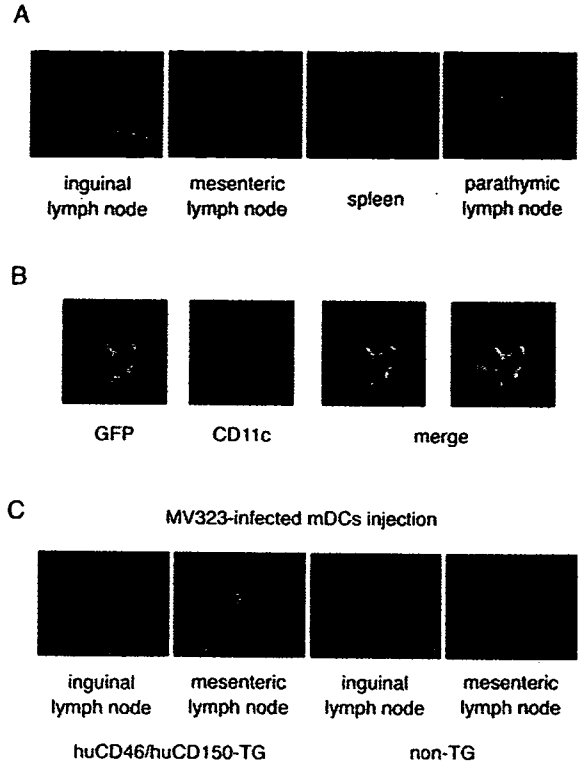

FIGURE 8. mDCs participate in systemic viral spreading. *A*, MV infection visualized in the triple mutant mice by in vivo inoculation of MV323GFP. Representative photographic images of GFP-positive organs in huCD46/huCD150 TG/IFNAR$^{-/-}$ mice are shown. At 48 h after i.p. injection of 10^5 $TCID_{50}$ of MV323GFP, the mice were dissected and tissues were directly examined under an inverted fluorescence microscope. Magnification, ×100. *B*, CD11c-positive cells reserve MV323GFP. Mesenteric lymph nodes were fixed with 4% paraformaldehyde and the sections were stained with PE-conjugated anti-mouse CD11c mAb (red). EGFP (green) and CD11c (red) were observed by confocal microscopy. Merging profiles are shown to the *right*. Magnification, ×400. *C*, MV infection visualized by transfer of MV-infected mDCs into IFNAR1$^{+/+}$ TG mice. mDCs prepared from huCD46/huCD150 TG/IFNAR$^{-/-}$ mice were infected with MV323GFP at MOI = 1. At 24 h later, MV323GFP-infected mDCs (1×10^6) were i.v. injected into huCD46/huCD150 TG, huCD46 TG, huCD150 TG, and non-TG mice (IFNAR1 is normal in all TG mice). Two days later, each mouse was dissected and tissues were directly examined under an inverted fluorescence microscope. Magnification, ×100. The results were confirmed by two additional experiments.

no positive cells were found in brain, thymus, lung, heart, liver, kidney or intestine.

We prepared sections from mesenteric lymph nodes, and stained with PE-conjugated anti-mouse CD11c mAb. As shown in Fig. 8*B*, GFP-positive and CD11c-positive cells merged in the lymph nodes. Thus, we speculated that MV-infected mDCs delivered viruses to local draining lymph nodes. To confirm this hypothesis, we i.v. transferred MV323GFP-infected mDCs (1×10^6 cells, MOI = 1) from huCD150/huCD46/IFNAR1$^{-/-}$ mice to huCD46/huCD150, huCD150, huCD46, or non-TG mice (IFNAR1 is normal in each mouse strain). Two days later, the affected mice were dissected and specified tissues were directly observed by inverted fluorescence microscope (Fig. 8*C*). In mesenteric and inguinal lymph nodes from huCD46/huCD150 TG and huCD150 TG mice, GFP-positive lesions were detected. No such lesions were observed in affected huCD46 TG and non-TG mice. Based on these results, we infer that in this model MV-infected mDCs facilitate establishing systemic MV infection. IFNAR1$^{-/-}$ mDCs allowing viral replication inside the cells, trigger successive viral delivering to lymph nodes.

Discussion

We generated TG mice that express MV receptors huCD46 and huCD150. The expression profiles and the distribution of these receptors in these mice were similar to those in humans. Mouse splenocytes from the double TG mice became susceptible to wild-type MV strains in vitro. Nevertheless, despite the fact that the TG mice expressed both huCD46/huCD150, they were highly resisted MV infection in vivo irrespective of the route of MV administration. huCD150 but not huCD46 was up-regulated in response to TLR stimulators and conferred high susceptibility to wild-type MV on mDCs. In vivo, normal CD11c-positive DCs were usually insensitive to wild-type MV infection, whereas these DCs turned susceptible to MV if their amplifiable IFN-inducing ability in response to MV infection was spoiled. Systemic MV infection was observed in the huCD46/huCD150 double TG mice with no IFNAR1 by direct MV injection or in the double TG mice with normal IFNAR1 by transfer of MV-infected mDC to them. Thus, in vivo MV permissiveness was accomplished when the IFNAR1 gene was simultaneously disrupted in DCs.

A crucial question remains elusive that this TG mice model with natural expression profile of huCD46 and huCD150 serve as a model for the investigation of human wild-type MV infection. Different from human, IFNAR1$^{-/-}$ mice induce basal production of IFN-β in response to IFN regulatory factor (IRF)-3 activation, but secondary amplifiable response is severely impaired (45, 46). Opposing to the results on human DC, mouse mDC more efficiently induce type I IFN in response to infection by wild-type MV than to infection by attenuated MV strains (Fig. 6). Wild-type MV strains barely induce amplified type I IFN production in human DCs, whereas attenuated strains robustly induce it (M. Taniguchi, N. Begum, and T. Seya, unpublished observation). Thus, pathogenicity of wild-type MV strains may not be reflected in our mouse model. MV strains, either wild-type or laboratory-adapted, appear to replicate well in human DCs if they induce only minute degrees of type I IFN (20). We would say that our mouse model in part reflects MV infection of humans whether we choose MV strains with lesser ability to induce IFN-β or choose to activate the secondary amplified type I IFN pathway. Further study is needed to confirm these issues.

Which of CD11c-positive DCs, mDCs, or pDCs play a major role in MV-mediated IFN induction is a critical question. Both mDC and pDC are CD11c-positive and possess the pathways that induce IFN type I in response to RNA viruses (47). Our infection study on mouse mDC is: 1) MV more prominently induces IFN-β than IFN-α in IC-infected double TG mice (Fig. 7, *C* and *D*); 2) double TG mice without IFNAR1 induced an extremely lower level of IFN-α as compared with the TG mice with normal IFNAR1 (Figs. 7*C* and 8*B*). This is true in human in which wild-type MV strains efficiently replicate in DCs and barely induce type I IFN (20, 43). Recent reports after the submission of our study clearly revealed that the MyD88-IRF-7 pathway in pDC is the main route of IFN-α induction in mice in several virus species (48, 49). Perhaps, mDC induces IFN-β via Toll-IL-1R homology domain-containing adapter molecule 1-mediated or RNA helicase RIG-I-mediated IRF-3 activation pathways, which is independent of MyD88-dependent IRF-7 activation pathway. We could test this issue regarding MV if the mouse IFN-α and IFN-β are separately determined by ELISA. At least blood cells barely induce the messages of type I IFN in response to MV infection (data not shown), and the role of pDC in our mouse MV infection model remain to

be settled. Further MV infection studies using mice disrupting either of the IFN-inducing pathways will be required to clarify the source of type I IFN in MV-infected TG mice.

Wild-type MV-H protein acts as a ligand for TLR2 (2) and up-regulates CD150 in human monocytes (50). Although in vitro analysis speculated that DC matures into a stage vulnerable to wild-type MV through TLR2 signaling (51), whether wild-type MV actually infects mDC in vivo remains undetermined. Our mouse model offers the possibility that the matured DC is the primary target of wild-type MV strains. Testing the role of TLR2 by MV-H protein stimulation in immature DC maturation is feasible in our model. Dysfunction of Ag-presenting capacity of DC through MV infection may be associated with modulation of TLR signaling by MV.

Previous reports suggested that MV efficiently infected human DC and suppressed DC-mediated allostimulatory lymphocyte proliferation (MLR) (52–54). Both wild-type and vaccine strains induce defective MLR response irrespective of the induction levels of type I IFNs. Testing MLR in intact vs MV-infected mDCs prepared from these TG mice will give us a hint to resolve DC-based immune suppression. The model may enable us to test the role of huCD150 and/or huCD46 on lymphocytes in association with infected mDCs.

A comparison of the double TG mice with huCD150 TG mice in their ability to produce differential cytokine levels suggests that huCD150 TG mice more efficiently induce all four cytokines tested than do huCD46/huCD150 TG mice (Fig. 6, *B–E*). The replication level of MV-H was high in huCD150 TG mice and relatively low in huCD46/huCD150 TG mice (Fig. 6*F*). The results suggest that CD46 expressed on mDCs acts as a negative regulator for wild-type MV replication. According to previous reports, mouse macrophages expressing human CD46 significantly resist MV infection (55). These cells produced high levels of NO and IFN-$\alpha\beta$ upon infection by MV (55, 56), suggesting that huCD46 enhances IFN-$\alpha\beta$ production in mouse macrophages. Thus, it is possible that simultaneous expression of huCD46 and huCD150 in mDC down-regulates MV replication. Alternatively, huCD46 in lymphocytes deliver negative or positive signal in lymphoproliferation depending on the type of tail sequences as reported previously (25, 26). There are two major isoforms of huCD46 with differential cytoplasmic tails (CYTs), CYT1 and CYT2 (25, 57). NO is induced in macrophages in a CYT1>CYT2 fashion (55, 58). In mouse lymphocytes from TG mice with either CYT1 or CYT2, differential functions of these isoforms were clearly observed (26). Relationship between the huCD46 isoforms and IFN-β production will be an issue to be tested in our model.

In human myeloid DCs, TLR3 and TLR8 participate in type I IFN production (59). Mouse mDCs lack TLR8 (60, 61). RIG-I participates in sensing viral infection inside the cells to activate a signaling pathway for induction of type I IFN (62). Yet, TLR3 may sense viral infection, as in West Nile virus entry into the brain (63). Human monocytes may express CD150 in the adenoid tissue to catch up inspired MV (50). Therefore, interpretation of differential responses between mouse mDC and human immature DC in wild *vs* vaccine strains need to take these recent findings into consideration. It is important to further analyze the natural intranasal infection of MV and its relationship to the properties of wild-type MV-infected CD11c-positive mDCs.

Our findings can be summarized as follows: 1) mouse CD11c-positive mDCs in huCD46/huCD150 double TG mice are barely susceptible to wild-type MV until IFNAR1 is depleted; 2) in the double TG mice with no IFNAR1, only CD11c-positive mDCs are vulnerable to MV at an early phase of infection in vivo; 3) robust IFN type I induction due to IFNAR1 by mDCs confers natural resistance to wild-type MV on mice; and 4) the huCD46/huCD150 double TG mouse when injected with MV-infected mDCs i.v. permits systemic infection by MV. Therefore, in this mouse model mDC carries MV to draining lymph nodes. Although the results were deduced from an artificial model case, the TG mice with or without IFNAR1 would be applicable for the study of MV-mediated initial IFN-β induction in mDC. With these mice, virus-mediated initial IFN-β inducing response and its related pathways involving IRF-3 and IRF-7 in mDCs may be critically analyzed. This is the first report on the generation of wild-type MV-sensitive mice.

Acknowledgments

We are grateful to Drs. K. Toyoshima, N. Inoue, M. Tanabe K. Funami, T. Tsujita (Osaka Medical Center for Cancer, Osaka, Japan), M. Ikawa (Osaka University), Y. Seto (Osaka City University), M. Kohanawa (Hokkaido University, Sapporo, Japan), and A. Takaoka (University of Tokyo, Tokyo, Japan) for helpful discussions. Thanks are also due to K. Shida, Y. Okuda, M. Sasai, A. Matsuo, and H. Masuda (Osaka Medical Center for Cancer) for helpful technical support. We thank Dr. M. A. Billeter (University of Zurich) for kindly providing p(+)MV2A plasmid and MV rescue system from cDNA and Dr. K. Takeuchi (Tsukuba University, Ibaragi, Japan) for kindly providing p(+)MV323 plasmid.

Disclosures

The authors have no financial conflict of interest.

References

1. Dorig, R. E., A. Marcil, A. Chopra, and C. D. Richardson. 1993. The human CD46 molecule is a receptor for measles virus (Edmonston strain). *Cell* 75: 295–305.
2. Naniche, D., G. Varior-Krishnan, F. Cervoni, T. F. Wild, B. Rossi, C. Rabourdin-Combe, and D. Gerlier. 1993. Human membrane cofactor protein (CD46) acts as a cellular receptor for measles virus. *J. Virol.* 67: 6025–6032.
3. Hsu, E. C., C. Iorio, F. Sarangi, A. A. Khine, and C. D. Richardson. 2001. CDw150(SLAM) is a receptor for a lymphotropic strain of measles virus and may account for the immunosuppressive properties of this virus. *Virology* 279: 9–21.
4. Tatsuo, H., N. Ono, K. Tanaka, and Y. Yanagi. 2000. SLAM (CDw150) is a cellular receptor for measles virus. *Nature* 406: 893–897.
5. Ono, N., H. Tatsuo, K. Tanaka, H. Minagawa, and Y. Yanagi. 2001. V domain of human SLAM (CDw150) is essential for its function as a measles virus receptor. *J. Virol.* 75: 1594–1600.
6. Tsujimura, A., K. Shida, M. Kitamura, M. Nomura, J. Takeda, H. Tanaka, M. Matsumoto, K. Matsumiya, A. Okuyama, Y. Nishimune, et al. 1998. Molecular cloning of a murine homologue of membrane cofactor protein (CD46): preferential expression in testicular germ cells. *Biochem. J.* 330(Pt. 1): 163–168.
7. Liebert, U. G., and D. Finke. 1995. Measles virus infections in rodents. *Curr. Top. Microbiol. Immunol.* 191: 149–166.
8. Rima, B. K., J. A. Earle, K. Baczko, P. A. Rota, and W. J. Bellini. 1995. Measles virus strain variations. *Curr. Top. Microbiol. Immunol.* 191: 65–83.
9. Horvat, B., P. Rivailler, G. Varior-Krishnan, A. Cardoso, D. Gerlier, and C. Rabourdin-Combe. 1996. Transgenic mice expressing human measles virus (MV) receptor CD46 provide cells exhibiting different permissivities to MV infections. *J. Virol.* 70: 6673–6681.
10. Oldstone, M. B., H. Lewicki, D. Thomas, A. Tishon, S. Dales, J. Patterson, M. Manchester, D. Homann, D. Naniche, and A. Holz. 1999. Measles virus infection in a transgenic model: virus-induced immunosuppression and central nervous system disease. *Cell* 98: 629–640.
11. Rall, G. F., M. Manchester, L. R. Daniels, E. M. Callahan, A. R. Belman, and M. B. Oldstone. 1997. A transgenic mouse model for measles virus infection of the brain. *Proc. Natl. Acad. Sci. USA* 94: 4659–4663.
12. Hahm, B., N. Arbour, D. Naniche, D. Homann, M. Manchester, and M. B. Oldstone. 2003. Measles virus infects and suppresses proliferation of T lymphocytes from transgenic mice bearing human signaling lymphocytic activation molecule. *J. Virol.* 77: 3505–3515.
13. Hahm, B., N. Arbour, and M. B. Oldstone. 2004. Measles virus interacts with human SLAM receptor on dendritic cells to cause immunosuppression. *Virology* 323: 292–302.
14. Manchester, M., D. S. Eto, A. Valsamakis, P. B. Liton, R. Fernandez-Munoz, P. A. Rota, W. J. Bellini, D. N. Forthal, and M. B. Oldstone. 2000. Clinical isolates of measles virus use CD46 as a cellular receptor. *J. Virol.* 74: 3967–3974.
15. Manchester, M., and G. F. Rall. 2001. Model systems: transgenic mouse models for measles pathogenesis. *Trends Microbiol.* 9: 19–23.
16. Mrkic, B., J. Pavlovic, T. Rulicke, P. Volpe, C. J. Buchholz, D. Hourcade, J. P. Atkinson, A. Aguzzi, and R. Cattaneo. 1998. Measles virus spread and pathogenesis in genetically modified mice. *J. Virol.* 72: 7420–7427.
17. Mrkic, B., B. Odermatt, M. A. Klein, M. A. Billeter, J. Pavlovic, and R. Cattaneo. 2000. Lymphatic dissemination and comparative pathology of recombinant measles viruses in genetically modified mice. *J. Virol.* 74: 1364–1372.

18. Peng, K. W., M. Frenzke, R. Myers, D. Soeffker, M. Harvey, S. Greiner, E. Galanis, R. Cattaneo, M. J. Federspiel, and S. J. Russell. 2003. Biodistribution of oncolytic measles virus after intraperitoneal administration into Ifnar-CD46Ge transgenic mice. *Hum. Gene Ther.* 14: 1565–1577.
19. Cocks, B. G., C. C. Chang, J. M. Carballido, H. Yssel, J. E. de Vries, and G. Aversa. 1995. A novel receptor involved in T-cell activation. *Nature* 376: 260–263.
20. Murabayashi, N., M. Kurita-Taniguchi, M. Ayata, M. Matsumoto, H. Ogura, and T. Seya. 2002. Susceptibility of human dendritic cells (DCs) to measles virus (MV) depends on their activation stages in conjunction with the level of CDw150: role of Toll stimulators in DC maturation and MV amplification. *Microbes Infect.* 4: 785–794.
21. Sidorenko, S. P., and E. A. Clark. 1993. Characterization of a cell surface glycoprotein IPO-3, expressed on activated human B and T lymphocytes. *J. Immunol.* 151: 4614–4624.
22. Karp, C. L. 1999. Measles: immunosuppression, interleukin-12, and complement receptors. *Immunol. Rev.* 168: 91–101.
23. Klagge, I. M., V. ter Meulen, and S. Schneider-Schaulies. 2000. Measles virus-induced promotion of dendritic cell maturation by soluble mediators does not overcome the immunosuppressive activity of viral glycoproteins on the cell surface. *Eur. J. Immunol.* 30: 2741–2750.
24. Schneider-Schaulies, S., S. Niewiesk, J. Schneider-Schaulies, and V. ter Meulen. 2001. Measles virus induced immunosuppression: targets and effector mechanisms. *Curr. Mol. Med.* 1: 163–181.
25. Kemper, C., A. C. Chan, J. M. Green, K. A. Brett, K. M. Murphy, and J. P. Atkinson. 2003. Activation of human $CD4^+$ cells with CD3 and CD46 induces a T-regulatory cell 1 phenotype. *Nature* 421: 388–392.
26. Marie, J. C., A. L. Astier, P. Rivailler, C. Rabourdin-Combe, T. F. Wild, and B. Horvat. 2002. Linking innate and acquired immunity: divergent role of CD46 cytoplasmic domains in T cell induced inflammation. *Nat. Immunol.* 3: 659–666.
27. Nishiguchi, M., M. Matsumoto, T. Takao, M. Hoshino, Y. Shimonishi, S. Tsuji, N. A. Begum, O. Takeuchi, S. Akira, K. Toyoshima, and T. Seya. 2001. *Mycoplasma fermentans* lipoprotein M161Ag-induced cell activation is mediated by Toll-like receptor 2: role of N-terminal hydrophobic portion in its multiple functions. *J. Immunol.* 166: 2610–2616.
28. Kimura, Y., and R. Yanagimachi. 1995. Intracytoplasmic sperm injection in the mouse. *Biol. Reprod.* 52: 709–720.
29. Perry, A. C., T. Wakayama, H. Kishikawa, T. Kasai, M. Okabe, Y. Toyoda, and R. Yanagimachi. 1999. Mammalian transgenesis by intracytoplasmic sperm injection. *Science* 284: 1180–1183.
30. Muller, U., U. Steinhoff, L. F. Reis, S. Hemmi, J. Pavlovic, R. M. Zinkernagel, and M. Aguet. 1994. Functional role of type I and type II interferons in antiviral defense. *Science* 264: 1918–1921.
31. Takeuchi, K., N. Miyajima, F. Kobune, and M. Tashiro. 2000. Comparative nucleotide sequence analyses of the entire genomes of B95a cell-isolated and Vero cell-isolated measles viruses from the same patient. *Virus Genes* 20: 253–257.
32. Kobune, F., H. Sakata, and A. Sugiura. 1990. Marmoset lymphoblastoid cells as a sensitive host for isolation of measles virus. *J. Virol.* 64: 700–705.
33. Radecke, F., P. Spielhofer, H. Schneider, K. Kaelin, M. Huber, C. Dotsch, G. Christiansen, and M. A. Billeter. 1995. Rescue of measles viruses from cloned DNA. *EMBO J.* 14: 5773–5784.
34. Takeda, M., K. Takeuchi, N. Miyajima, F. Kobune, Y. Ami, N. Nagata, Y. Suzaki, Y. Nagai, and M. Tashiro. 2000. Recovery of pathogenic measles virus from cloned cDNA. *J. Virol.* 74: 6643–6647.
35. Tsuji, S., M. Matsumoto, O. Takeuchi, S. Akira, I. Azuma, A. Hayashi, K. Toyoshima, and T. Seya. 2000. Maturation of human dendritic cells by cell wall skeleton of *Mycobacterium bovis* bacillus Calmette-Guerin: involvement of Toll-like receptors. *Infect. Immun.* 68: 6883–6890.
36. Akazawa, T., H. Masuda, Y. Saeki, M. Matsumoto, K. Takeda, K. Tsujimura, K. Kuzushima, T. Takahashi, I. Azuma, S. Akira, K. Toyoshima, and T. Seya. 2004. Adjuvant-mediated tumor regression and tumor-specific cytotoxic response are impaired in MyD88-deficient mice. *Cancer Res.* 64: 757–764.
37. Kaisho, T., O. Takeuchi, T. Kawai, K. Hoshino, and S. Akira. 2001. Endotoxin-induced maturation of MyD88-deficient dendritic cells. *J. Immunol.* 166: 5688–5694.
38. Inaba, K., M. Pack, M. Inaba, H. Sakuta, F. Isdell, and R. M. Steinman. 1997. High levels of a major histocompatibility complex II-self peptide complex on dendritic cells from the T cell areas of lymph nodes. *J. Exp. Med.* 186: 665–672.
39. Miyagawa, S., S. Mikata, H. Tanaka, M. Ikawa, K. Kominami, T. Seya, Y. Nishimune, R. Shirakura, and M. Okabe. 1997. The regulation of membrane cofactor protein (CD46) expression by the 3′ untranslated region in transgenic mice. *Biochem. Biophys. Res. Commun.* 233: 829–833.
40. Johnstone, R. W., B. E. Loveland, and I. F. McKenzie. 1993. Identification and quantification of complement regulator CD46 on normal human tissues. *Immunology* 79: 341–347.
41. Inoue, N., A. Fukui, H. Oshiumi, M. Matsumoto, and T. Seya. 1999. Method for production of human CD46 transgenic mice. *Host Defense* 8: 27 (*Abstr.*).
42. Kemper, C., M. Leung, C. B. Stephensen, C. A. Pinkert, M. K. Liszewski, R. Cattaneo, and J. P. Atkinson. 2001. Membrane cofactor protein (MCP: CD46) expression in transgenic mice. *Clin. Exp. Immunol.* 124: 180–189.
43. Naniche, D., A. Yeh, D. Eto, M. Manchester, R. M. Friedman, and M. B. Oldstone. 2000. Evasion of host defenses by measles virus: wild-type measles virus infection interferes with induction of α/β interferon production. *J. Virol.* 74: 7478–7484.
44. Tanabe, M., M. Kurita-Taniguchi, K. Takeuchi, M. Takeda, M. Shingai, M. Ayata, H. Ogura, M. Matsumoto, and T. Seya. 2003. Mechanism of up-regulation of human Toll-like receptor (TLR) 3 secondary to infection of measles virus attenuated strains. *Biochem. Biophys. Res. Commun.* 311: 39–48.
45. Taniguchi, T., and A. Takaoka. 2002. The interferon-α/β system in antiviral responses: a multimodal machinery of gene regulation by the IRF family of transcription factors. *Curr. Opin. Immunol.* 14: 111–116.
46. Jiang, Z., T. W. Mak, G. Sen, and X. Li. 2004. Toll-like receptor 3-mediated activation of NF-κB and IRF3 diverges at Toll-IL-1 receptor domain-containing adapter inducing IFN-β. *Proc. Natl. Acad. Sci. USA* 101: 3533–3538.
47. Sato, A., and A. Iwasaki. 2004. Induction of antiviral immunity requires Toll-like receptor signaling in both stromal and dendritic cell compartments. *Proc. Natl. Acad. Sci. USA* 101: 16274–16279.
48. Kawai, T., S. Sato, K. J. Ishii, C. Coban, H. Hemmi, M. Yamamoto, K. Terai, M. Matsuda, J. Inoue, S. Uematsu, et al. 2004. Interferon-α induction through Toll-like receptors involves a direct interaction of IRF7 with MyD88 and TRAF6. *Nat. Immunol.* 10: 1061–1068.
49. Honda, K., H. Yanai, H. Negishi, M. Asagiri, M. Sato, T. Mizutani, N. Shimada, Y. Ohba, A. Takaoka, N. Yoshida, and T. Taniguchi. 2005. IRF-7 is the master regulator of type-I interferon-dependent immune responses. *Nature* 434: 772–777.
50. Minagawa, H., K. Tanaka, N. Ono, H. Tatsuo, and Y. Yanagi. 2001. Induction of the measles virus receptor SLAM (CD150) on monocytes. *J. Gen. Virol.* 82(Pt. 12): 2913–2917.
51. Bieback, K., E. Lien, I. M. Klagge, E. Avota, J. Schneider-Schaulies, W. P. Duprex, H. Wagner, C. J. Kirschning, V. Ter Meulen, and S. Schneider-Schaulies. 2002. Hemagglutinin protein of wild-type measles virus activates Toll-like receptor 2 signaling. *J. Virol.* 76: 8729–8736.
52. Fugier-Vivier, I., C. Servet-Delprat, P. Rivailler, M. C. Rissoan, Y. J. Liu, and C. Rabourdin-Combe. 1997. Measles virus suppresses cell-mediated immunity by interfering with the survival and functions of dendritic and T cells. *J. Exp. Med.* 186: 813–823.
53. Grosjean, I., C. Caux, C. Bella, I. Berger, F. Wild, J. Banchereau, and D. Kaiserlian. 1997. Measles virus infects human dendritic cells and blocks their allostimulatory properties for $CD4^+$ T cells. *J. Exp. Med.* 186: 801–812.
54. Schlender, J., J. J. Schnorr, P. Spielhoffer, T. Cathomen, R. Cattaneo, M. A. Billeter, V. ter Meulen, and S. Schneider-Schaulies. 1996. Interaction of measles virus glycoproteins with the surface of uninfected peripheral blood lymphocytes induces immunosuppression in vitro. *Proc. Natl. Acad. Sci. USA* 93: 13194–13194.
55. Hirano, A., Z. Yang, Y. Katayama, J. Korte-Sarfaty, and T. C. Wong. 1999. Human CD46 enhances nitric oxide production in mouse macrophages in response to measles virus infection in the presence of γ interferon: dependence on the CD46 cytoplasmic domains. *J. Virol.* 73: 4776–4785.
56. Katayama, Y., A. Hirano, and T. C. Wong. 2000. Human receptor for measles virus (CD46) enhances nitric oxide production and restricts virus replication in mouse macrophages by modulating production of α/β interferon. *J. Virol.* 74: 1252–1257.
57. Seya, T., and S. Nagasawa. 2001. CD46: membrane cofactor protein of complement and a measles virus receptor. In *Encyclopedia of Molecular Medicine*. T. E. Creighton, ed. John Wiley & Sons, Inc. New York, NY, p. 628.
58. Hirano, A., M. Kurita-Taniguchi, Y. Katayama, M. Matsumoto, T. C. Wong, and T. Seya. 2002. Ligation of human CD46 with purified complement C3b or $F(ab')_2$ of monoclonal antibodies enhances isoform-specific interferon γ-dependent nitric oxide production in macrophages. *J. Biochem.* 132: 83–91.
59. Jurk, M., F. Heil, J. Vollmer, C. Schetter, A. M. Krieg, H. Wagner, G. Lipford, and S. Bauer. 2002. Human TLR7 or TLR8 independently confer responsiveness to the antiviral compound R-848. *Nat. Immunol.* 3: 499.
60. Heil, F., H. Hemmi, H. Hochrein, F. Ampenberger, C. Kirschning, S. Akira, G. Lipford, H. Wagner, and S. Bauer. 2004. Species-specific recognition of single-stranded RNA via Toll-like receptor 7 and 8. *Science* 303: 1526–1529.
61. Coccia, E. M., M. Severa, E. Giacomini, D. Monneron, M. E. Remoli, I. Julkunen, M. Cella, R. Lande, and G. Uze. 2004. Viral infection and Toll-like receptor agonists induce a differential expression of type I and λ interferons in human plasmacytoid and monocyte-derived dendritic cells. *Eur. J. Immunol.* 34: 796–805.
62. Yoneyama, M., M. Kikuchi, T. Natsukawa, N. Shinobu, T. Imaizumi, M. Miyagishi, K. Taira, S. Akira, and T. Fujita. 2004. The RNA helicase RIG-I has an essential function in double-stranded RNA-induced innate antiviral responses. *Nat. Immunol.* 5: 730–737.
63. Wang, T., T. Town, L. Alexopoulou, J. F. Anderson, E. Fikrig, and R. A. Flavell. 2004. Toll-like receptor 3 mediates West Nile virus entry into the brain causing lethal encephalitis. *Nat. Med.* 10: 1366–1373.
64. Kurita-Taniguchi, M., A. Fukui, K. Hazeki, A. Hirano, S. Tsuji, M. Watanabe, M. Matsumoto, S. Ueda, and T. Seya. 2000. Functional modulation of human macrophages through CD46 (measles virus receptor): production of IL-12 p40 and nitric oxide in association with recruitment of SHP-1 to CD46. *J. Immunol.* 165: 5143–5152.

J. Biochem. **139**, 921–930 (2006)
doi:10.1093/jb/mvj104

Proteomic Profiling of Lipid Droplet Proteins in Hepatoma Cell Lines Expressing Hepatitis C Virus Core Protein

Shigeko Sato[1], Masayoshi Fukasawa[1,*], Yoshio Yamakawa[1], Tohru Natsume[2], Tetsuro Suzuki[3], Ikuo Shoji[3], Hideki Aizaki[3], Tatsuo Miyamura[3] and Masahiro Nishijima[1,†]

[1]Department of Biochemistry and Cell Biology and [3]Department of Virology II, National Institute of Infectious Diseases, Tokyo 162-8640; and [2]National Institute of Advanced Industrial Science and Technology (AIST), Biological Information Research Center, Tokyo 135-0064

Received February 7, 2006; accepted April 4, 2006

Hepatitis C virus (HCV) core protein has been suggested to play crucial roles in the pathogeneses of liver steatosis and hepatocellular carcinomas due to HCV infection. Intracellular HCV core protein is localized mainly in lipid droplets, in which the core protein should exert its significant biological/pathological functions. In this study, we performed comparative proteomic analysis of lipid droplet proteins in core-expressing and non-expressing hepatoma cell lines. We identified 38 proteins in the lipid droplet fraction of core-expressing (Hep39) cells and 30 proteins in that of non-expressing (Hepswx) cells by 1-D-SDS-PAGE/MALDI-TOF mass spectrometry (MS) or direct nanoflow liquid chromatography–MS/MS. Interestingly, the lipid droplet fraction of Hep39 cells had an apparently lower content of adipose differentiation–related protein and a much higher content of TIP47 than that of Hepswx cells, suggesting the participation of the core protein in lipid droplet biogenesis in HCV-infected cells. Another distinct feature is that proteins involved in RNA metabolism, particularly DEAD box protein 1 and DEAD box protein 3, were detected in the lipid droplet fraction of Hep39 cells. These results suggest that lipid droplets containing HCV core protein may participate in the RNA metabolism of the host and/or HCV, affecting the pathopoiesis and/or virus replication/production in HCV-infected cells.

Key words: ADRP, DEAD box protein, hepatitis C virus, lipid droplet, TIP47.

Abbreviations: HCV, hepatitis C virus; HCC, hepatocellular carcinoma; MS, mass spectrometry; DNLC, direct nanoflow liquid chromatography; HRP, horseradish peroxidase; ADRP, adipose differentiation–related protein; DDX1, DEAD box protein 1; DDX3, DEAD box protein 3.

Hepatitis C virus (HCV) is a major causative agent of chronic hepatitis (*1*, *2*). Persistent HCV infection, which occurs in more than 70% of infected patients, is strongly associated with the development of liver steatosis, which involves the accumulation of intracellular lipid droplets, cirrhosis, and hepatocellular carcinomas (HCC) (*3*, *4*). Since more than 170 million people in the world are currently infected with HCV (*1*), and there is no cure that is completely effective, understanding the mechanism by which HCV induces serious liver diseases is one of the most important global public health issues. HCV, a member of the *Flaviviridae* family, possesses a single-stranded, positive-sense RNA genome of ~9.6 kb (*5*). The HCV genome has a single open reading frame that codes for a large precursor polyprotein of ~3,000 amino acids that is processed into at least 10 individual proteins by host and viral proteases (*6*).

HCV core protein, the product of the N-terminal portion of the polyprotein, generated upon cleavage at the endoplasmic reticulum by signal peptidase and signal peptide peptidase (*7*, *8*), forms the nucleocapsid of an HCV virion (*9*). Interestingly, in addition to its function as a structural protein, the core protein exhibits activities leading host cells to lipogenic and malignant transformation *in vitro* (*10–12*). Moreover, transgenic mice expressing HCV core protein developed liver steatosis and HCC (*13*, *14*), suggesting an important role of the core protein in these diseases. Many studies have shown that HCV core protein substantially affects various cellular regulatory processes, such as gene transcription (*15–17*) and signal transduction pathways (*12*, *18–23*), and interacts with a variety of host proteins (*12*, *18*, *19*, *22*, *24–34*), but it is not clear what activities/molecules are practically relevant to the pathogeneses of HCV (core)-derived liver steatosis and HCC. Extensive screenings for genes/proteins exhibiting differences in cellular expression by cDNA microarray (*35–40*) or proteome analysis (*41*, *42*) have also been tried for HCV-related HCC. Although various genes/proteins were identified, further studies are required to identify the molecules eventually involved in the pathogenesis of HCV-related HCC.

In host cells, HCV core protein is distributed mainly in lipid droplets and the endoplasmic reticulum (*7*, *10*, *43–46*), in which the core protein is predicted to exert its significant biological/pathological functions. In this study, we thus focused on HCV core protein and lipid droplets, and

*To whom correspondence should be addressed. Tel: +81-3-5285-1111, Fax: +81-3-5285-1157, E-mail: fuka@nih.go.jp
†Present address: Department of Clinical Pharmacy, Faculty of Pharmaceutical Sciences, Doshisha Women's College of Liberal Arts, Kyoto 610-0395.

performed comparative targeted proteomic analysis of the lipid droplet proteins in HCV core-expressing and non-expressing hepatoma cell lines using two strategies: conventional 1-D-SDS-PAGE/MALDI-TOF mass spectrometry (MS) and automated high-throughput direct nanoflow liquid chromatography (DNLC)–MS/MS. We found prominent differences in the protein compositions of lipid droplets between HCV core-expressing and non-expressing hepatoma cell lines.

MATERIALS AND METHODS

Cell Lines—The human hepatoma HepG2 cell line constitutively expressing HCV core protein (Hep39) was established as described previously (*47*). Another HepG2 cell line transfected with expression vector pcEF321swxneo without the HCV core protein insert (Hepswx) was used as a mock control (*47*). Both cell lines were plated on collagen-coated dishes (Asahi Techno Glass, Tokyo, Japan) and maintained in the normal culture medium [DMEM supplemented with 10% fetal bovine serum, 100 units/ml Penicillin G, 100 μg/ml streptomycin sulfate, and 1 mg/ml G418 (Sigma, St. Louis, MO, USA)] under a 5% CO_2 atmosphere at 37°C.

Lipid Droplet Preparation—Hepswx and Hep39 cells were seeded at 4×10^6 cells/dish (150 mm, inner diameter) in 25 ml of normal culture medium and cultured for one day. For efficient formation of lipid droplets by cells, cholesterol (final 20 μg/ml) and oleic acid (final 400 μM)/fatty acid-free BSA (final 60 μM) complex, prepared as stock solutions of 5 mg/ml cholesterol in ethanol and 10 mM oleic acid/1.5 mM BSA in PBS, respectively, were added to the medium. Each cell line was further incubated for 48–72 h at 37°C. For proteomic analysis of lipid droplet proteins, confluent monolayers of Hepswx and Hep39 cells in fifteen cell culture dishes (150 mm, inner diameter) were harvested by scraping and pelleted by centrifugation ($200 \times g$ for 5 min at 4°C). After being washed with PBS three times, each cell pellet was resuspended in 10 mM Tris-HCl buffer, pH 7.5, containing 0.25 M sucrose and Complete™, EDTA-free (Roche, Mannheim, Germany) to achieve a final volume equal to five times the volume of the cell pellet (*i.e.* a 20% cell suspension). The cell suspension was homogenized with a ball-bearing homogenizer (*48*), and then centrifuged at $800 \times g$ for 5 min at 4°C. One milliliter of each post-nuclear supernatant fraction was layered under 2 ml of 10 mM Tris-HCl buffer, pH 7.5, containing 0.15 M NaCl (TN-buffer). After centrifugation at $100,000 \times g$ for 60 min at 4°C, the lipid droplet fraction, *i.e.* the distinct white band on the top of the preparation, was collected with a pipetman. The floating lipid droplet fraction was diluted with 3.5 ml of TN-buffer and then re-purified by centrifugation ($100,000 \times g$ for 30 min at 4°C). This washing step was repeated three times. Lipid droplets in the floating fractions in both cells were enriched up to more than 500-fold compared with those in the total cell lysates as estimated by their protein contents. The amounts of lipid droplets isolated from Hepswx and Hep39 cells were nearly the same. The purified lipid droplet fractions (~0.1 mg of protein per ml) were stored at −80°C until use. The purity of the lipid droplet fractions was verified by microscopic and immunoblot (Fig. 1) analyses. Adipose differentiation-related protein (ADRP), a known lipid droplet protein, was significantly enriched in the lipid droplet fractions of Hepswx and Hep39 cells (Fig. 1). Other organelle marker proteins, such as nucleoporin p62 for the nucleus, prohibitin for the mitochondria, fatty acid synthase for the cytoplasm, GM130 for the Golgi apparatus, EEA1 for the early endosome, or annexin II for the plasma membrane, were not detected in the lipid droplet fractions of either cells (Fig. 1). Small amounts of calnexin, a marker of the endoplasmic reticulum, which is a major organelle, were detected in the lipid droplet fractions of both cells to a similar extent. Although we did not detect calnexin in the lipid droplet fractions by proteomic analysis (see Tables 1 and 2), the lipid droplet fractions of both cells could be contaminated with a small amount of endoplasmic reticulum.

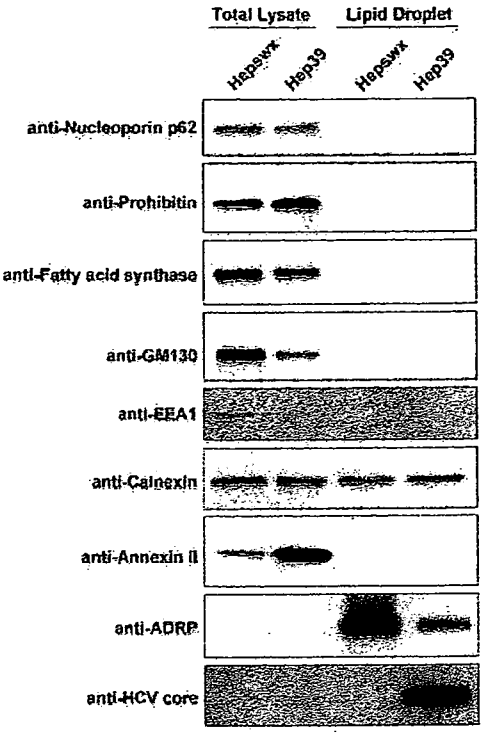

Fig. 1. **Immunoblot analysis of lipid droplet fractions in Hepswx and Hep39 cells using antibodies against various organelle markers.** Total cell lysates and lipid droplet fractions (1.5 μg of protein per lane in the case of anti-ADRP; 5 μg of protein per lane in others) from Hepswx and Hep39 cells were analyzed by immunoblotting with the indicated antibodies.

1-D-SDS-PAGE/MALDI-TOF MS Analysis—The lipid droplet fraction (30 μg protein) of each cell line was fractionated in a 10% SDS–polyacrylamide gel, and the gel was stained with Coomassie Brilliant Blue. The protein bands were excised from the gel and subjected to in-gel trypsin digestion. The tryptic peptide mixtures were analyzed by MALDI-TOF MS as described previously (*49*). Prior to MALDI-TOF MS analysis, the peptide mixtures were desalted using C18 Zip Tips (Millipore, Billerica, MA, USA) according to the manufacturer's instructions. The peptide data were collected in the reflection mode and with positive polarity, using a saturated solution of

Table 1. **Lipid droplet proteins identified in Hepswx and Hep39 cells by means of 1-D-SDS-PAGE/MALDI-TOF MS.**

Protein	Molecular mass (kDa) (calc.)	Accession No.	SDS band No.[a]	
			Hepswx	Hep39
PAT family proteins				
Adipose differentiation–related protein (ADRP)	48.1	34577059	5	21
Cargo selection protein/TIP47	47.0	20127486		22
Lipid metabolism				
Acyl CoA synthetase long chain family member 3	80.4	42794752	4	18
Cytochrome b_5 reductase	34.3	4503327	9	26
Lanosterol synthase	83.3	4808278	4	18
NAD(P)-dependent steroid dehydrogenase-like; H105e3	41.9	8393516	8	25
Retinal short-chain dehydrogenase/reductase retSDR2	33.0	7705905	10	27
Cytosolic phospholipase A_2	85.2	1352707		14
Rab GTPases				
Rab1A	22.7	4758988	13	30
Rab1B	22.2	23396834	13	30
Rab5C	23.5	38258923	11	28
Rab7	23.5	34147513	12	29
RNA metabolism/binding				
DEAD box protein 1 (DDX1)	82.9	6919862		16
DEAD box protein 3 (DDX3)	73.2	3023628		18
HC56/gemin 4	118.8	10945430		15
Other/unknown proteins				
BiP protein	70.9	14916999	3	17
CGI-49 protein	46.9	7705767	6	23
Heat shock protein gp96 precursor	90.2	15010550	2	14
Ancient ubiquitous protein 1	41.4	31712024	7	
Major vault protein	99.3	15990478	1	
Apoptosis-inducing factor–homologous mitochondrion-associated inducer of death	40.5	13543964		24
KIAA0887 protein	52.4	4240263		21
Protein disulfide-isomerase [EC 5.3.4.1] ER60 precursor	56.7	1085373		20
Transport-secretion protein 2.1	57.7	9663151		19
HCV core protein	20.6	974345		31

[a]Band numbers correspond to those in Fig. 2.

α-cyano-4-hydroxycinnamic acid (Sigma) in 50% acetonitrile and 0.1% trifluoroacetic acid as the matrix. Spectra were obtained using a Voyager DE-STR MALDI-TOF mass spectrometer (PE Biosystems, Foster City, CA, USA). Internal calibration was performed with adrenocorticotropic hormone, fragment 18–39 (Sigma), and bradykinin fragment (Sigma). The data base–fitting program MS-Fit available at the WWW site of the University of California, San Francisco (prospector.ucsf.edu/ucsfhtml3.4/msfit.htm) was used to interpret the MS spectra of protein digests (*50*).

DNLC-MS/MS Analysis—The lipid droplet fraction (10 μg protein) of each cell line was first delipidated by chloroform–methanol extraction as originally described (*51*). Two volumes of chloroform and 1 volume of methanol were mixed with 0.8 volume of the lipid droplet fraction. Then, 1 volume of chloroform and 1 volume of water were added to the mixture, and the mixture was vortexed for 30 s, and centrifuged at 10,000 × *g* for 5 min at room temperature. The resulting organic (lower) phase was removed. The aqueous (upper) phase and interface, containing all the lipid droplet proteins, was lyophilized. The delipidated lipid droplet proteins were digested with endoproteinase Lys-C, and the resulting peptides were analyzed by DNLC-MS/MS as described (*52*, *53*).

Cell Fractionation—All manipulations were performed at 4°C or on ice. After being washed with PBS, confluent monolayers of Hepswx and Hep39 cells were harvested by scraping and pelleted by centrifugation (200 × *g*, 5 min). The precipitated cells were homogenized with a ball-bearing homogenizer in 10 mM Tris-HCl buffer, pH 7.5, containing 0.25 M sucrose, and Complete™, EDTA-free. After centrifugation of the lysate at 800 × *g* for 5 min, the cytosolic fraction (100,000 × *g* supernatant) and membrane fraction (100,000 × *g* precipitate) were separated from the post-nuclear supernatant fraction by centrifugation at 100,000 × *g* for 60 min. The membrane fraction was resuspended in TN-buffer and then re-purified twice by centrifugation. The protein concentrations of these preparations were determined with BCA protein assay reagents (Pierce Biotechnology, Rockford, IL, USA) using BSA as a standard.

Immunoblot Analysis—Equivalent amounts of proteins from Hepswx and Hep39 cells were separated in a 10 or 12.5% SDS–polyacrylamide gel and then electrophoretically transferred to a polyvinylidene difluoride membrane. The membranes were blocked overnight at 4°C or 30 min at room temperature in TBS containing 0.1% Tween 20 and 5% skim milk. The blots were probed with a mouse

Table 2. **Lipid droplet proteins identified in Hepswx and Hep39 cells by means of DNLC-MS/MS.**

Protein	Accession No.	Molecular mass (kDa) (calc.)	Matched peptide sequence	
			Hepswx[a]	Hep39[a]
PAT family proteins				
Adipose differentiation–related protein (ADRP)	34577059	48.1	+ TITSVAMTSALPIIQK DAVTTTVTGAK EVSDSLLTSSK	+ TITSVAMTSALPIIQK DAVTTTVTGAK EVSDSLLTSSK
Cargo selection protein / TIP47	20127486	47.0	+ VSGAQEMVSSAK	+ VSGAQEMVSSAK
Lipid metabolism				
Acyl-CoA synthetase long-chain family member 3	42794752	80.4	+ VLSEAAISASLEK	+ ELTELARK
Cytochrome b_5 reductase	4503327	34.2	+ DILLRPELEELRNK	+ SNPIIRTVK
Gastric-associated differentially-expressed protein YA61P	6970062	14.9	+ AIGLVVPSLTGK	+ AIGLVVPSLTGK
Retinal short-chain dehydrogenase/ reductase retSDR2	7705905	33.0	+ HGLEETAAK	+ FDAVIGYK
Sterol carrier protein 2–related form, 58.85K	86717	58.8	+ LQNLQLQPGNAK	+ LQNLQLQPGNAK
Acyl-CoA synthetase long-chain family member 4	4758332	74.4	+ SDQSYVISFVVPNQK	
Fatty acid binding protein 5	4557581	15.2	+ ELGVGIALRK	
Hydroxysteroid (17-beta) dehydrogenase 4	4504505	79.7		+ NHPMTPEAVK
Rab GTPases				
Rab1A	4758988	22.6	+[b] QWLQEIDRYASENVNK RMGPGATAGGAEK	+ RMGPGATAGGAEK
Rab1B	23396834	22.1	+[b] QWLQEIDRYASENVNK	+ RMGPGAASGGERPNLK
Rab7	34147513	23.5	+ NNIPYFETSAK	+ ATIGADFLTK
Rab18	20809384	22.9	+ HSMLFIEASAK	+ ILIIGESGVGK
Rab10	12654157	22.5	+ LLLIGDSGVGK	
Rab11	4758986	24.5	+ VVLIGDSGVGK	
Rab8	539607	23.6		+ IRTIELDGK
RNA metabolism/binding				
DEAD box protein 1 (DDX1)	6919862	82.4		+ FGFGFGGTGK
DEAD box protein 3 (DDX3)	3023628	73.2		+ GVRHTMMFSATFPK
IGF-II mRNA-binding protein 3	30795212	63.7		+ EGATIRNITK
Ribosomal protein L29	14286258	17.8		+ AQAAAPASVPAQAPK
Other/unknown proteins				
Apoptosis-inducing factor homologous mitochondrion-associated inducer of death	13543964	40.5	+ EVTLIHSQVALADK	+ EVTLIHSQVALADK
BiP protein	14916999	72.3	+ SQIFSTASDNQPTVTIK	+ VYEGERPLTK
Hypothetical protein DKFZp586A0522.1	7512845	28.2	+ LQHIQAPLSWELVRPH-IYGYAVK	+ RELFSNLQEFAGPSGK
Prolyl 4-hydroxylase, beta subunit	20070125	57.1	+ VHSFPTLK	+ AEGSEIRLAK
Ancient ubiquitous protein 1	31712024	41.4	+ GTQSLPTASASK	
Heat shock protein gp96 precursor	15010550	90.2	+ FAFQAEVNRMMK	
Hypothetical protein FLJ21820	11345458	37.3	+ DIYGLNGQIEHK	
Molecule possessing ankyrin repeats induced by lipopolysaccharide	38173790	78.1	+ CLIQMGAAVEAK	
Ubiquitin-conjugating enzyme E2G 2, isoform 1	15079469	18.6	+ RLMAEYK	
CGI-49 protein	7705767	46.9		+ AGGVFTPGAAFSK
DILV594	37182139	31.4		+ RELFSQIK
Hypothetical protein DKFZp564F0522.1—human (fragment)	7512734	33.1		+ ILRTSSGSIREK
Hypothetical protein HSPC117	7657015	55.2		+ EQLAQAMFDHIPVGVGSK
Tumor protein D52–like 2 isoform e	40805860	22.2		+ TQETLSQAGQK
Vesicle amine transport protein 1	15679945	41.9		+ VVTYGMANLLTGPK

[a]+, detected. [b]This peptide sequence is present in both Rab1A and Rab1B.

monoclonal anti-ADRP antibody (PROGEN Biotechnik GmbH, Heidelberg, Germany) (1:25), a guinea pig polyclonal anti-TIP47 antibody (PROGEN Biotechnik GmbH) (1:250), a mouse monoclonal anti-HCV core protein antibody (Anogen, Ontario, Canada) (1: 1,000), a mouse monoclonal anti-DDX1 antibody (Pharmingen, San Diego, CA, USA) (1:500), or a rabbit polyclonal anti-DDX3 antibody (antibody custom-made by Invitrogen, CA, USA) (1:500) for 90 min at room temperature. The blots were then incubated with horseradish peroxidase (HRP)–conjugated goat anti-rabbit IgG (BIO-RAD), HRP-conjugated goat anti-mouse IgG (BIO-RAD), or HRP-conjugated goat anti-guinea pig IgG (ICN Pharmaceuticals, Aurora, OH, USA) at 1:2,000 dilution for 60 min. Detection of immunoreactive proteins was performed with an ECL system (Amersham Biosciences Corp., Piscataway, NJ, USA).

RESULTS

Proteomic Analysis of Lipid Droplets by 1-D-SDS-PAGE/MALDI-TOF MS—Lipid droplet proteins from control (HCV core non-expressing) Hepswx cells and HCV core–expressing Hep39 cells were separated by 10% SDS-PAGE, and the protein bands were visualized by Coomassie Brilliant Blue staining (Fig. 2). In each cell line ~30 bands were seen. The visible bands (areas) were excised from the gels, trypsinized, and analyzed by MALDI-TOF MS. Among the 31 bands, we identified 25 proteins: 15 proteins in Hepswx cells and 23 proteins in Hep39 cells (Fig. 2 and Table 1). Thirteen of the 25 proteins were detected in both types of cell. The lipid droplet proteins found in both Hepswx and Hep39 cells could be categorized into four groups: (1) PAT family proteins, *i.e.* ADRP and TIP47; (2) multiple molecules involved in lipid metabolism; (3) several Rab GTPases; and (4) other/unknown proteins (Table 1). In addition, Hep39 cells contained another group of proteins involved in RNA metabolism/binding (Table 1).

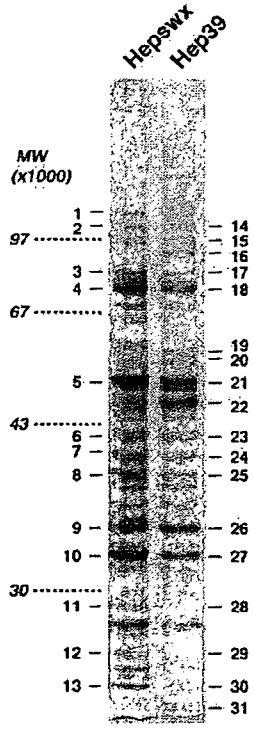

Fig. 2. **Signature SDS-PAGE patterns of the lipid droplet fractions of Hepswx and Hep39 cells.** Proteins in the purified lipid droplet fractions (30 μg of protein per lane) of Hepswx cells and Hep39 cells were separated in a 10% SDS–polyacrylamide gel, and visualized by Coomassie Brilliant Blue staining. The 31 numbered bands were excised from the gel, subjected to in-gel trypsin digestion, and processed for MALDI-TOF-MS. Molecular weights (MW) are given to the left of the gel.

Proteomic Analysis of Lipid Droplets by DNLC-MS/MS—Some protein bands in Fig. 2 could not be identified, probably due to the restricted separation capacity of 1-D-SDS-PAGE (*i.e.* multiple proteins migrating to the same area). We had, however, difficulty in applying 2-DE to the separation of lipid droplet proteins because of their hydrophobic characteristics. We then tried a new LC-based MS strategy. Lipid droplet fractions from Hepswx and Hep39 cells were delipidated and then digested with Lys-C. The resulting peptide mixtures were directly analyzed using a DNLC-MS/MS system (*52*). We identified 36 lipid droplet proteins: 24 proteins in Hepswx cells and 27 proteins in Hep39 cells (Table 2). Twenty-three lipid droplet proteins were newly identified with this system. Fifteen proteins detected in both cell lines were classified into four categories (Table 2) as in the case of 1-D-SDS-PAGE/MALDI-TOF MS analysis. A group of proteins involved in RNA metabolism/binding was also found only in Hep39 cells (Table 2).

Proteins Exhibiting Differences in Their Association with Lipid Droplets Due to HCV Core Protein Expression—SDS-PAGE patterns of lipid droplet proteins were similar but revealed several distinct differences in protein composition between Hepswx and Hep39 cells (Fig. 2). The most remarkable differences were seen in the bands corresponding to PAT family proteins. The amount of ADRP, a major PAT family protein in lipid droplets in the liver (*54*, *55*), and likely to be the most abundant lipid droplet protein in Hepswx cells (Fig. 2, band 5), seemed to be less in HCV core–expressing Hep39 cells (Fig. 2, band 21). On the other hand, TIP47, which is also known to be a PAT family protein in lipid droplets (*56*, *57*), was detected as a major protein only in Hep39 cells (Fig. 2, band 22, and Table 1). To confirm these findings, the contents of ADRP and TIP47 in the lipid droplet fractions of Hepswx and Hep39 cells were examined by immunoblot analysis with specific antibodies. The lipid droplet fraction of HCV core–expressing Hep39 cells showed an apparently lower content of ADRP and a much higher content of TIP47 than the levels in Hepswx cells (Fig. 3).

Next we examined the cellular distributions of ADRP and TIP47 in Hepswx and Hep39 cells by cell fractionation. ADRP was highly concentrated in the lipid droplet fractions of both cells, even though the content in the lipid droplets was much lower in Hep39 cells than in Hepswx cells (Fig. 4). ADRP was not detected in post-nuclear supernatant fractions or in either the cytosol or membrane fractions, probably because of low expression levels in these cells or low affinity of the anti-ADRP antibody we used

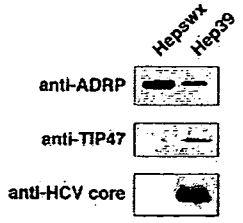

Fig. 3. **The lipid droplet fraction of Hep39 cells contains less ADRP, but more TIP47, than Hepswx cells.** Lipid droplet fractions (1.5 μg of protein per lane) from Hepswx and Hep39 cells were analyzed by immunoblotting with the indicated antibodies.

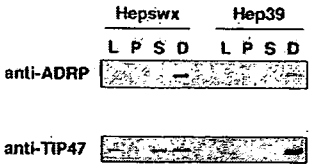

Fig. 4. **Subcellular localization of ADRP and TIP47 in Hepswx and Hep39 cells.** Hepswx and Hep39 cells were fractionated into post-nuclear supernatant (lane L), 100,000 × *g* precipitate (lane P), 100,000 × *g* supernatant (lane S), and lipid droplet (lane D) fractions as described in "MATERIALS AND METHODS." Ten micrograms of protein was processed for gel electrophoresis, and then analyzed by immuonoblotting with anti-ADRP and anti-TIP47 antibodies.

(Fig. 4). The mRNA expression level of ADRP in Hep39 cells was less than half that in Hepswx cells (data not shown), consistent with the immunoblot data shown in Fig. 4. These results suggest that the lower ADRP content in the lipid droplet fraction of Hep39 cells is due to a low expression level of ADRP. In contrast, Hep39 cells had much more TIP47 in the lipid droplet fraction (Figs. 3 and 4, lanes D), but the cellular TIP47 content of Hep39 cells was not more than that in Hepswx cells (Fig. 4, lanes L). Besides the lipid droplet fraction, the cytosolic fraction of Hepswx cells was found to contain TIP47 at a substantial level, while the cytosolic fraction of Hep39 cells did not (Fig. 4, lanes S). These results indicate that the intracellular distribution of TIP47 shifts drastically from the cytosol to lipid droplets in HCV core–expressing Hep39 cells.

Another obvious difference between Hepswx and Hep39 cells in Fig. 2 is the presence of a specific ~85 kDa band (Fig. 2, band 16) in Hep39 cells, which was identified as DEAD box protein 1 (DDX1), a DEAD box protein family member, by 1-D-SDS-PAGE/MALDI-TOF MS analysis (Table 1). DNLC-MS/MS analysis also supported the existence of DDX1 in the lipid droplet fraction of Hep39 cells (Table 2). In addition, DEAD box protein 3 (DDX3), another DEAD box protein family member, was also detected in the lipid droplet fraction of Hep39 cells by means of the two different strategies used for proteomic analysis (Tables 1 and 2), suggesting that DDX3 is a major lipid droplet protein in Hep39 cells. To verify the association of DDX 1 and DDX3 with lipid droplets in Hep39 cells, immunoblot analysis was carried out. Figure 5 shows that DDX 1 and DDX 3 exist in the lipid droplet fraction of HCV core-expressing Hep39 cells, but not Hepswx cells. These results imply the special pathological functions of DDX1 and DDX3 in lipid droplets in HCV core–expressing cells.

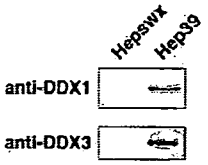

Fig. 5. **Hep39 cells, but not Hepswx cells, have DDX1 and DDX3 in the lipid droplet fraction.** Lipid droplet fractions (0.5 μg of protein per lane) in Hepswx and Hep39 cells were analyzed by immunoblotting with anti-DDX1 and anti-DDX3 antibodies.

DISCUSSION

To analyze lipid droplet proteins, we performed proteomic analysis by means of 1-D-SDS-PAGE/MALDI-TOF MS and automated DNLC-MS/MS, and identified 25 and 36 proteins, respectively (Tables 1 and 2). Many more lipid droplet proteins were identified by DNLC-MS/MS, and 22 major proteins separated by 1-D-SDS-PAGE (Fig. 2, bands, 2, 3, 4, 5, 7, 9, 10, 12, 13, 16, 17, 18, 21, 22, 24, 26, 27, 29, and 30) and detected on MALDI-TOF MS analysis were also detected on DNLC-MS/MS analysis. These results indicate that DNLC-MS/MS is a very sensitive and reliable system as well as a high-throughput method. Particularly, DNLC-MS/MS would be a powerful system for exhaustive proteomic analysis of protein mixtures/complexes (up to ~100 proteins) such as lipid droplets.

In our targeted proteomic study, we identified a total of 48 lipid droplet proteins: 30 proteins in control Hepswx cells, 38 proteins in HCV core–expressing Hep39 cells, and 20 proteins in both cell lines. The resident lipid droplet proteins were classified into four groups (Tables 1 and 2), consistent with the recently reported data obtained on proteomic analysis of lipid droplet proteins in other cell lines (*58–60*). In addition, multiple proteins, such as the sterol carrier protein 2–related form, fatty acid binding protein 5, and apoptosis-inducing factor homologous mitochondrion-associated inducer of death, were newly identified as lipid droplet proteins in this study. These accumulated data obtained on proteomic analysis will be useful for understanding the biogenesis and functions of lipid droplets about which little is yet known.

A prominent effect of the expression of HCV core protein on the composition of lipid droplet proteins was observed among the PAT family proteins, i.e. ADRP and TIP47. HCV core–expressing Hep39 cells contained much less ADRP in the lipid droplet fraction (Fig. 3), probably because of the lower cellular expression level and the lack of induction of expression upon lipid loading (data not shown). In contrast, a substantial amount of TIP47 was associated with the lipid droplet fraction of Hep39 cells (Fig. 3). Perilipin, a structural protein of lipid droplets in adipocytes, ADRP, and TIP47, termed PAT family proteins (*61*), share extensive amino acid sequence similarity (*61–63*), suggesting a common biological function in lipid droplet formation. For example, the transition in surface protein composition of lipid droplets from ADRP to perilipin occurs during adipocyte differentiation (*64*). Thus, TIP47 might replace ADRP

on the lipid droplets in Hep39 cells. Cellular TIP47 was not up-regulated in Hep39 cells, resulting in a reduction of TIP47 in the cytosolic fraction (Fig. 4). Since TIP47, originally identified as having the ability to interact with the mannose 6-phosphate/IGF-II receptor (*63*), appears to be essential for the endocytic recycling system (*65–67*), the altered distribution of cellular TIP47 in Hep39 cells could affect intracellular membrane trafficking pathways. Consistent with this assumption, our preliminary results showed that the rate of protein secretion from cells was apparently slower for Hep39 cells than Hepswx cells (unpublished data). Patients chronically infected with HCV (*68*) and HCV core–transgenic mice (*69*) exhibit decreased levels of plasma very low density lipoproteins secreted from the liver, also suggesting interference with intracellular membrane trafficking (secretion pathways) by HCV core proteins. We currently speculate that the reduction in cellular ADRP expression mediated by HCV core protein causes the accumulation of TIP47 in lipid droplets as a substitute, and that the resulting depletion of TIP47 in the cytosol could cause the impairment of intracellular membrane trafficking, followed by the cellular accumulation of membrane lipids and consequent lipid droplet formation. Although further studies remain to be done to confirm these possibilities, we suggest that HCV core protein influences not only the biogenesis of lipid droplets but also intracellular membrane trafficking.

Another interesting finding in this study is that Hep39 cells, unlike Hepswx cells, contain DEAD box proteins, DDX1 and DDX3, as major lipid droplet proteins (Figs. 2 and 5). On the basis of the results of studies involving yeast two-hybrid assays, DDX3 has been shown to be able to interact with HCV core protein, and studies involving immunofluorescent microscopy have revealed that DDX3 is distributed in cytosolic spots such as lipid droplets (*27, 70, 71*). These results, together with our present findings, suggest that DDX3 is associated with lipid droplets via HCV core proteins located on lipid droplets. In addition to DDX1 and DDX3, which possess ATPase/RNA helicase activities (*27, 72, 73*), several other proteins involved in RNA metabolism/binding, including HC56/gemin 4 and IGF-II mRNA–binding protein 3, were also detected in the lipid droplet fraction of HCV core-expressing Hep39 cells (Tables 1 and 2). Recently Dvorak *et al.* reported that RNA itself can be associated with lipid droplets in human mast cells (*74*). Taken together, these data strongly suggest that lipid droplets containing HCV core proteins may participate in the RNA metabolism of the host and/or HCV in HCV-infected cells. Furthermore, the findings that DDX1 is overexpressed in cell lines derived from tumors such as retinoblastomas and neuroblastomas (*75*), and that cellular expression of DDX3 induces anchorage-independent cell growth (*76*) suggest the involvement of DDX1 and DDX3 in carcinogenesis.

Some groups recently reported profiles of mRNAs up- or down-regulated by expression of the HCV core protein (*77–79*), but these mRNAs included no molecules identified as lipid droplet proteins in this study. Since lipid droplets are a minor organelle in cells, it might be difficult to detect changes in the mRNA expression levels of lipid droplet proteins. The merits of targeted proteomic study are that it is possible to focus on minor cellular fractions, and also to detect changes in the intracellular distributions of proteins. Actually, the mRNA expression levels of TIP47, DDX1, and DDX3 did not change in Hep39 cells (data not shown).

We identified many other lipid droplet proteins found in either Hepswx or Hep39 cells, but their biological functions remain mostly unknown (Tables 1 and 2). Elucidation of the biological functions of these proteins will lead to an advanced understanding of the pathogeneses of HCV-derived liver diseases.

This work was supported by Grants-in-Aid from the Ministry of Health, Labor and Welfare; the program for the Promotion of Fundamental Studies in Health Sciences of the Organization for Drug ADR Relief, R&D Promotion, and Product Review of Japan; the TAKEDA SCIENCE FOUNDATION; and the Integrated Proteomics System Project for Pioneer Research on Genome the Frontier from the Ministry of Education, Culture, Sports, Science & Technology of Japan.

REFERENCES

1. Choo, Q.L., Kuo, G., Weiner, A.J., Overby, L.R., Bradley, D.W., and Houghton, M. (1989) Isolation of a cDNA clone derived from a blood-borne non-A, non-B viral hepatitis genome. *Science* **244**, 359–362
2. Kuo, G., Choo, Q.L., Alter, H.J., Gitnick, G.L., Redeker, A.G., Purcell, R.H., Miyamura, T., Dienstag, J.L., Alter, M.J., Stevens, C.E., Tegtmeier, G.E., Bonino, F., Colombo, M., Lee, W.-S., Kuo, C., Berger, K., Shuster, J.R., Overby, L.R., Bradley, D.W., and Houghton, M. (1989) An assay for circulating antibodies to a major etiologic virus of human non-A, non-B hepatitis. *Science* **244**, 362–364
3. Saito, I., Miyamura, T., Ohbayashi, A., Harada, H., Katayama, T., Kikuchi, S., Watanabe, Y., Koi, S., Onji, M., Ohta, Y., Choo, Q.-L., Houghton, M., and Kuo, G. (1990) Hepatitis C virus infection is associated with the development of hepatocellular carcinoma. *Proc. Natl. Acad. Sci. USA* **87**, 6547–6549
4. Kiyosawa, K., Sodeyama, T., Tanaka, E., Gibo, Y., Yoshizawa, K., Nakano, Y., Furuta, S., Akahane, Y., Nishioka, K., Purcell, R.H., and Alter, H.J. (1990) Interrelationship of blood transfusion, non-A, non-B hepatitis and hepatocellular carcinoma: analysis by detection of antibody to hepatitis C virus. *Hepatology* **12**, 671–675
5. Bartenschlager, R. and Lohmann, V. (2000) Replication of hepatitis C virus. *J. Gen. Virol.* **81**, 1631–1648
6. Grakoui, A., Wychowski, C., Lin, C., Feinstone, S.M., and Rice, C.M. (1993) Expression and identification of hepatitis C virus polyprotein cleavage products. *J. Virol.* **67**, 1385–1395
7. McLauchlan, J., Lemberg, M.K., Hope, G., and Martoglio, B. (2002) Intramembrane proteolysis promotes trafficking of hepatitis C virus core protein to lipid droplets. *EMBO J.* **21**, 3980–3988
8. Okamoto, K., Moriishi, K., Miyamura, T., and Matsuura, Y. (2004) Intramembrane proteolysis and endoplasmic reticulum retention of hepatitis C virus core protein. *J. Virol.* **78**, 6370–6380
9. Santolini, E., Migliaccio, G., and La Monica, N. (1994) Biosynthesis and biochemical properties of the hepatitis C virus core protein. *J. Virol.* **68**, 3631–3641
10. Barba, G., Harper, F., Harada, T., Kohara, M., Goulinet, S., Matsuura, Y., Eder, G., Schaff, Z., Chapman, M.J., Miyamura, T., and Brechot, C. (1997) Hepatitis C virus core protein shows a cytoplasmic localization and associates to cellular lipid storage droplets. *Proc. Natl. Acad. Sci. USA* **94**, 1200–1205
11. Ray, R.B., Lagging, L.M., Meyer, K., and Ray, R. (1996) Hepatitis C virus core protein cooperates with ras and transforms

primary rat embryo fibroblasts to tumorigenic phenotype. *J. Virol.* **70**, 4438–4443
12. Yoshida, T., Hanada, T., Tokuhisa, T., Kosai, K., Sata, M., Kohara, M., and Yoshimura, A. (2002) Activation of STAT3 by the hepatitis C virus core protein leads to cellular transformation. *J. Exp. Med.* **196**, 641–653
13. Moriya, K., Yotsuyanagi, H., Shintani, Y., Fujie, H., Ishibashi, K., Matsuura, Y., Miyamura, T., and Koike, K. (1997) Hepatitis C virus core protein induces hepatic steatosis in transgenic mice. *J. Gen. Virol.* **78**, 1527–1531
14. Moriya, K., Fujie, H., Shintani, Y., Yotsuyanagi, H., Tsutsumi, T., Ishibashi, K., Matsuura, Y., Kimura, S., Miyamura, T., and Koike, K. (1998) The core protein of hepatitis C virus induces hepatocellular carcinoma in transgenic mice. *Nat. Med.* **4**, 1065–1067
15. Kim, D.W., Suzuki, R., Harada, T., Saito, I., and Miyamura, T. (1994) Trans-suppression of gene expression by hepatitis C viral core protein. *Jpn. J. Med. Sci. Biol.* **47**, 211–220
16. Ray, R.B., Steele, R., Meyer, K., and Ray, R. (1997) Transcriptional repression of p53 promoter by hepatitis C virus core protein. *J. Biol. Chem.* **272**, 10983–10986
17. Shrivastava, A., Manna, S.K., Ray, R., and Aggarwal, B.B. (1998) Ectopic expression of hepatitis C virus core protein differentially regulates nuclear transcription factors. *J. Virol.* **72**, 9722–9728
18. Chen, C.M., You, L.R., Hwang, L.H., and Lee, Y.H. (1997) Direct interaction of hepatitis C virus core protein with the cellular lymphotoxin-beta receptor modulates the signal pathway of the lymphotoxin-beta receptor. *J. Virol.* **71**, 9417–9426
19. Zhu, N., Khoshnan, A., Schneider, R., Matsumoto, M., Dennert, G., Ware, C., and Lai, M.M. (1998) Hepatitis C virus core protein binds to the cytoplasmic domain of tumor necrosis factor (TNF) receptor 1 and enhances TNF-induced apoptosis. *J. Virol.* **72**, 3691–3697
20. Tsuchihara, K., Hijikata, M., Fukuda, K., Kuroki, T., Yamamoto, N., and Shimotohno, K. (1999) Hepatitis C virus core protein regulates cell growth and signal transduction pathway transmitting growth stimuli. *Virology* **258**, 100–107
21. You, L.R., Chen, C.M., and Lee, Y.H. (1999) Hepatitis C virus core protein enhances NF-kappaB signal pathway triggering by lymphotoxin-beta receptor ligand and tumor necrosis factor alpha. *J. Virol.* **73**, 1672–1681
22. Aoki, H., Hayashi, J., Moriyama, M., Arakawa, Y., and Hino, O. (2000) Hepatitis C virus core protein interacts with 14–3-3 protein and activates the kinase Raf-1. *J. Virol.* **74**, 1736–1741
23. Yoshida, H., Kato, N., Shiratori, Y., Otsuka, M., Maeda, S., Kato, J., and Omata, M. (2001) Hepatitis C virus core protein activates nuclear factor kappa B-dependent signaling through tumor necrosis factor receptor-associated factor. *J. Biol. Chem.* **276**, 16399–16405
24. Matsumoto, M., Hsieh, T.Y., Zhu, N., VanArsdale, T., Hwang, S.B., Jeng, K.S., Gorbalenya, A.E., Lo, S.Y., Ou, J.H., Ware, C.F., and Lai, M.M. (1997) Hepatitis C virus core protein interacts with the cytoplasmic tail of lymphotoxin-beta receptor. *J. Virol.* **71**, 1301–1309
25. Hsieh, T.Y., Matsumoto, M., Chou, H.C., Schneider, R., Hwang, S.B., Lee, A.S., and Lai, M.M. (1998) Hepatitis C virus core protein interacts with heterogeneous nuclear ribonucleoprotein K. *J. Biol. Chem.* **273**, 17651–17659
26. Sabile, A., Perlemuter, G., Bono, F., Kohara, K., Demaugre, F., Kohara, M., Matsuura, Y., Miyamura, T., Brechot, C., and Barba, G. (1999) Hepatitis C virus core protein binds to apolipoprotein AII and its secretion is modulated by fibrates. *Hepatology* **30**, 1064–1076
27. You, L.R., Chen, C.M., Yeh, T.S., Tsai, T.Y., Mai, R.T., Lin, C.H., and Lee, Y.H. (1999) Hepatitis C virus core protein interacts with cellular putative RNA helicase. *J. Virol.* **73**, 2841–2853
28. Jin, D.Y., Wang, H.L., Zhou, Y., Chun, A.C., Kibler, K.V., Hou, Y.D., Kung, H., and Jeang, K.T. (2000) Hepatitis C virus core protein-induced loss of LZIP function correlates with cellular transformation. *EMBO J.* **19**, 729–740
29. Wang, F., Yoshida, I., Takamatsu, M., Ishido, S., Fujita, T., Oka, K., and Hotta, H. (2000) Complex formation between hepatitis C virus core protein and p21Waf1/Cip1/Sdi1. *Biochem. Biophys. Res. Commun.* **273**, 479–484
30. Otsuka, M., Kato, N., Lan, K., Yoshida, H., Kato, J., Goto, T., Shiratori, Y., and Omata, M. (2000) Hepatitis C virus core protein enhances p53 function through augmentation of DNA binding affinity and transcriptional ability. *J. Biol. Chem.* **275**, 34122–34130
31. Tsutsumi, T., Suzuki, T., Shimoike, T., Suzuki, R., Moriya, K., Shintani, Y., Fujie, H., Matsuura, Y., Koike, K., and Miyamura, T. (2002) Interaction of hepatitis C virus core protein with retinoid X receptor alpha modulates its transcriptional activity. *Hepatology* **35**, 937–946
32. Hosui, A., Ohkawa, K., Ishida, H., Sato, A., Nakanishi, F., Ueda, K., Takehara, T., Kasahara, A., Sasaki, Y., Hori, M., and Hayashi, N. (2003) Hepatitis C virus core protein differently regulates the JAK-STAT signaling pathway under interleukin-6 and interferon-gamma stimuli. *J. Biol. Chem.* **278**, 28562–28571
33. Ohkawa, K., Ishida, H., Nakanishi, F., Hosui, A., Ueda, K., Takehara, T., Hori, M., and Hayashi, N. (2004) Hepatitis C virus core functions as a suppressor of cyclin-dependent kinase-activating kinase and impairs cell cycle progression. *J. Biol. Chem.* **279**, 11719–11726
34. Alisi, A., Giambartolomei, S., Cupelli, F., Merlo, P., Fontemaggi, G., Spaziani, A., and Balsano, C. (2003) Physical and functional interaction between HCV core protein and the different p73 isoforms. *Oncogene* **22**, 2573–2580
35. Okabe, H., Satoh, S., Kato, T., Kitahara, O., Yanagawa, R., Yamaoka, Y., Tsunoda, T., Furukawa, Y., and Nakamura, Y. (2001) Genome-wide analysis of gene expression in human hepatocellular carcinomas using cDNA microarray: identification of genes involved in viral carcinogenesis and tumor progression. *Cancer Res.* **61**, 2129–2137
36. Shirota, Y., Kaneko, S., Honda, M., Kawai, H.F., and Kobayashi, K. (2001) Identification of differentially expressed genes in hepatocellular carcinoma with cDNA microarrays. *Hepatology* **33**, 832–840
37. Iizuka, N., Oka, M., Yamada-Okabe, H., Mori, N., Tamesa, T., Okada, T., Takemoto, N., Tangoku, A., Hamada, K., Nakayama, H., Miyamoto, T., Uchimura, S., and Hamamoto, Y. (2002) Comparison of gene expression profiles between hepatitis B virus- and hepatitis C virus-infected hepatocellular carcinoma by oligonucleotide microarray data on the basis of a supervised learning method. *Cancer Res.* **62**, 3939–3944
38. Iizuka, N., Oka, M., Yamada-Okabe, H., Mori, N., Tamesa, T., Okada, T., Takemoto, N., Hashimoto, K., Tangoku, A., Hamada, K., Nakayama, H., Miyamoto, T., Uchimura, S., and Hamamoto, Y. (2003) Differential gene expression in distinct virologic types of hepatocellular carcinoma: association with liver cirrhosis. *Oncogene* **22**, 3007–3014
39. Smith, M.W., Yue, Z.N., Geiss, G.K., Sadovnikova, N.Y., Carter, V.S., Boix, L., Lazaro, C.A., Rosenberg, G.B., Bumgarner, R.E., Fausto, N., Bruix, J., and Katze, M.G. (2003) Identification of novel tumor markers in hepatitis C virus-associated hepatocellular carcinoma. *Cancer Res.* **63**, 859–864
40. Smith, M.W., Yue, Z.N., Korth, M.J., Do, H.A., Boix, L., Fausto, N., Bruix, J., Carithers, R.L., Jr., and Katze, M.G. (2003) Hepatitis C virus and liver disease: global transcriptional profiling and identification of potential markers. *Hepatology* **38**, 1458–1467
41. Takashima, M., Kuramitsu, Y., Yokoyama, Y., Iizuka, N., Toda, T., Sakaida, I., Okita, K., Oka, M., and Nakamura, K. (2003) Proteomic profiling of heat shock protein 70 family members as biomarkers for hepatitis C virus-related hepatocellular carcinoma. *Proteomics* **3**, 2487–2493